Fuel 295 (2021) 120544

Contents lists available at ScienceDirect

Fuel

journal homepage: www.elsevier.com/locate/fuel

Full Length Article

Alternative fuels co-fired with natural gas in the pre-calciner of a cement plant: Energy and material flows

Daya R. Nhuchhen *, Song P. Sit, David B. Layzell

Canadian Energy Systems Analysis Research (CESAR) Initiative, University of Calgary, Calgary, AB, Canada

ARTICLE INFO

Keywords:
Natural gas-fired cement plant
Alternative fuels
Co-firing
Thermal energy flow
Energy demand
GHG emissions
Regression

ABSTRACT

Cement-making is an energy-intensive industrial process that contributes 8% of the global CO_2 emissions. This study develops a thermal energy flow model (TEF) for 4200 tonnes of clinker per day, a natural gas-fired cement plant in which 50% of the pre-calciner energy requirements can be supplied by alternative fuels (AF) including biomass, plastics, etc. The TEF shows that the lower heating value (LHV dry), oxygen content (dry basis) and moisture content of the AF, as well as the flue gas oxygen concentration [O_2] needed for complete combustion, affect the thermal energy intensity (TEI) and total air demand (AD). Compared to the reference system fueled by natural gas (NG) that burns completely at 1% [O_2] in flue gas, all AFs require more total air and thermal energy demand, especially when the solid AFs need a higher [O_2] in the flue gas (typically 3%) to ensure complete combustion. Due to the higher carbon (C) intensity, co-firing AFs could increase the total CO_2 emissions by 1% to 18%. For the wood dust with 100% biogenic C, 50% NG replacement in pre-calciner could avoid 55.5 and 43.1 $kgCO_2$/t clinker at 1% and 3% [O_2] in flue gas respectively, an equivalent of 7.5% and 5.8% decrease in total GHG emissions relative to the reference case. Results of the TEF model from 24 diverse AFs were used to generate regressions that link fuel properties and flue gas oxygen requirement with TEI, making it possible to compare highly diverse AFs for their likely performance in the clinker-making.

1. Introduction

The global cement sector accounts for about 8% of anthropogenic greenhouse gas (GHG) emissions [1] and product demand is expected to grow by 12–23% by 2050 [2]. About 90% of the GHG emissions [3] are associated with the production of clinker (clk) which makes up about 65% of cement by weight [2].

Global average CO_2 emissions are 831 $kgCO_2$/t clk [2], about 560 $kgCO_2$/t clk of which comes from the conversion of calcium carbonate to calcium oxide, known as process emissions (PE). The rest of the GHG footprint (~271 $kgCO_2$/t clk) is associated with energy emissions (EE) to drive the thermal process of the clinker-making process.

In most cement plants, coal or pet-coke provides the primary fuel and has a carbon intensity of about 97 $kgCO_2$ per GJ_{LHV} [4], resulting in the EE of about 281 to 611 kg CO_2/t clk depending upon the thermal energy demand of the facility (range from 2.9 to 6.3 GJ/t clk) [5]. Some coal or pet-coke fired cement plants [6–8] incorporate waste-derived alternative fuels (AF) to reduce costs [9] and eliminate waste streams. If the AF replacing coal or pet-coke are bio-based, GHGs also can be reduced. Keeping organic materials out of landfill sites is also known to eliminate the emission of methane, a potent GHG [10].

Tsiliyannis [11] provided a detailed thermal model describing mass and energy flow in a cement plant where AFs were co-fired with coal and analyzed the impact of AF on clinker productions and GHG emissions. Rahman et al. [12] extended this work using ASPEN Plus process modeling. Ariyaratne et al. [6] and Tsiliyannis [13] also used thermal energy models to quantify the benefits of oxygen enrichment in a cement plant where AFs were co-fired with coals.

Natural gas (NG) can also be used for clinker production as a low carbon alternative (carbon intensity of 56 $kgCO_2/GJ_{LHV}$) [4] to coal or pet-coke. One benefit of NG is that complete combustion can be obtained with relatively low excess air supply (i.e. flue gas oxygen concentration of about 1% by molar basis), while solid fuels like coal or pet-coke often need more excess air, resulting in a higher flue gas oxygen concentration (2% to 7%) to achieve complete combustion [6,13–15]. Akhtar and co-workers [14] provided a computational analysis that compared the combustion behavior of coal and NG in the kiln and pre-calciner of a cement plant while Atsonios et al. [16] reported on how different fuels

* Corresponding author.
E-mail addresses: drnhuchhen@gmail.com, daya.nhuchhen@ucalgary.ca (D.R. Nhuchhen).

https://doi.org/10.1016/j.fuel.2021.120544
Received 2 November 2020; Received in revised form 21 February 2021; Accepted 22 February 2021

including NG firing in a cement plant would impact the technology used for carbon capture process for geological storage.

To the knowledge of the authors, no studies have been published on the use of AFs in natural gas-fired cement plant. This study is focused on addressing this knowledge gap.

In the province of Alberta in Canada, NG is available at a low price so it is used by one cement plant (LafargeHolcim Inc, Exshaw, Alberta) to achieve a CO_2 emissions intensity for clinker production of 738 $kgCO_2/t$ clk. The plant must report on its GHG emissions under the province's Technology Innovation and Emissions Reduction (TIER) regulations [17]. The regulation allocates an emissions intensity benchmark of 776 $kgCO_2/t$ clk including both process and energy emissions. A facility exceeding the benchmark will pay $30/$tCO_2e$ rising to $50/$tCO_2e$ in 2022 and to $170/$tCO_2e$ in 2030 [18]. Alternatively, a facility performing below the benchmark can earn emissions reduction offset credits. Despite the low emission intensity of their NG-fired cement plant, LafargeHolcim is interested in exploring the potential for AFs to reduce both the fuel cost and the CO_2 emissions intensity of clinker production [19].

In this study, a thermal energy flow (TEF) model describes the operation of a natural gas-fired cement plant without and with 24 different waste-derived AFs providing 50% of the energy requirements for the pre-calciner. The study explores how the embedded elemental oxygen content (O), lower heating value (LHV) and moisture content (MC) of the AFs impacted their thermal energy intensity (TEI, GJ_{LHV}/t clk), air demand (AD, Nm^3/t clk) and CO_2 emissions intensity ($kgCO_2/t$ clk). Since the studied AFs are solid fuels and may require more excess air to ensure complete combustion, the TEF model also assesses the effect of flue gas oxygen concentrations ($[O_2]$) on TEI, AD and GHG emissions of the clinker production process.

The findings of the TEF model are also used to generate the regression equation that relates the AFs fuel properties and the required flue gas oxygen concentration with the TEI requirements for an NG-fired cement plant.

2. Methodology

2.1. Properties of alternative fuels

Details on the lower heating values (LHV) and elemental composition of NG and 24 different AFs obtained from the published literature [20] are arranged in the order of their carbon intensity (Table 1). It also shows biogenic carbon content published in the literature [21–23]. Three bolded AFs: High-density polythene (HDPE), railway ties 2 (RT2) and wood dust (WD) with 0%, 74%, and 100% biogenic carbon [22], respectively were selected to examine the details of the energy and material flows in this study.

2.2. Process flow diagram

A simplified process flow diagram for the 4200 tonnes clinker per day cement plant that is the focus of this study is shown in Fig. 1. It includes a 4-stage raw meal preheater, an inline pre-calciner, rotary kiln, and clinker cooler. NG and/or AFs in the pre-calciner and only NG in the rotary kiln are supplied to drive the calcining and sintering reactions. Raw materials (RM) with 3% moisture (as received basis) are milled in a vertical rotating mill and dried with the help of the flue gas and exhaust vent air before being fed into the preheater tower. The key plant-specific operational temperatures and other parameters for the cement plant are shown in Fig. 1 and the shaded portion indicates the major changes that

Table 1
Characteristics of solid alternative fuels [20].

Alternative fuels	LHV (MJ/kg - Dry basis)	Elemental analysis (%Wt. - Dry basis)								Carbon intensity (kg CO_2/GJ_{LHV})	Biogenic C (% of total C)
		C	H	O	N	Ar	S	Cl	Ash		
Natural gas (NG)[a]	47.57	74.15	24.58	0.01	1.26	0.00	0.00	0.00	0.00	57	0
Rubber chips (RC)	35.94	65.84	10.86	5.77	0.78	0.00	1.53	0.82	14.40	67	0
High-density polythene (HDPE)	**43.29**	**86.10**	**13.00**	**0.90**	**0.00**	**0.00**	**0.00**	**0.00**	**0.00**	**73**	**0**
TV back plate (TVBP)	37.73	82.20	7.21	2.96	0.99	0.00	0.03	5.39	1.22	80	0
Electronic plastic waste 1 (EPW1)	30.73	67.40	6.84	7.66	2.94	0.00	0.11	4.44	10.60	80	0
Carpet grains (CG)	20.34	45.09	5.78	30.06	2.78	0.00	0.11	0.00	16.20	81	0
Electronic plastic waste 2 (EPW2)	25.13	56.60	5.97	8.24	2.81	0.00	0.10	7.38	18.90	83	0
Spent coffee (SC)	25.29	57.00	7.60	32.90	2.10	0.00	0.10	0.00	0.30	83	100
Asphalt shingles (AS)	13.48	31.64	3.55	20.81	0.17	0.00	1.43	0.00	42.40	86	20[b]
Waste tire (WT)	32.89	82.79	6.99	7.67	0.67	0.00	1.56	0.28	0.06	92	0
Soybean oil cake (SOC)	15.38	38.80	5.74	41.86	6.64	0.00	0.00	0.00	6.96	92	100
Brewing industries waste (BIW)	20.23	51.10	6.87	32.51	4.66	0.00	0.44	0.02	4.40	93	100
Coffee husk (CH)	18.80	49.40	6.10	41.12	0.81	0.00	0.07	0.00	2.50	96	100
Shuttering wood (SW)	17.14	45.46	5.51	37.86	1.79	0.00	0.03	0.00	9.36	97	100
Wood dust (WD)	**16.06**	**43.14**	**4.84**	**32.34**	**0.66**	**0.00**	**0.51**	**0.13**	**18.37**	**98**	**100**
Bone meal (BM)	18.28	49.16	7.04	16.73	10.21	0.00	0.63	0.97	15.26	99	100
Railway ties 1 (RT1)	19.73	53.50	5.50	39.78	0.30	0.00	0.01	0.01	0.90	99	74[b]
Painted wood (PW)	18.40	49.90	5.43	42.02	0.46	0.00	0.04	0.07	2.08	99	52[c]
Telephone poles (TP)	20.33	55.66	6.02	34.51	0.44	0.00	0.56	0.40	2.41	100	53[c]
Railway ties 2 (RT2)	**20.37**	**56.11**	**6.06**	**35.83**	**0.47**	**0.00**	**0.12**	**0.04**	**1.37**	**101**	**74[b]**
Lignin from wood (LW)	21.94	62.17	5.89	31.11	0.16	0.00	0.06	0.00	0.62	104	100
Cardboard (CB)	15.39	44.52	5.68	41.18	0.10	0.00	0.12	0.00	8.40	106	100[d]
Empty fruit brunches palm oil (PO)	15.56	45.53	5.46	43.39	0.46	0.00	0.04	0.00	5.12	107	100
Textile (T)	14.03	41.11	6.96	50.90	0.01	0.00	0.84	0.00	0.20	107	100[b]
Plywood (P)	15.89	49.53	6.17	41.98	0.58	0.00	0.03	0.00	1.80	114	54[c]

[a] Composition of NG: Methane-96.9%; Ethane-2.3%; Propane-0.06%; Iso-Butane-0.004%; Normal Butane-0.004%; Traces amount of Hexane; Nitrogen 0.7%; Carbon dioxide-0.005%, and lower heating value: 35 MJ/Nm^3 (Provided by the industry partner of this study).
[b] [22];
[c] [21];
[d] [23].

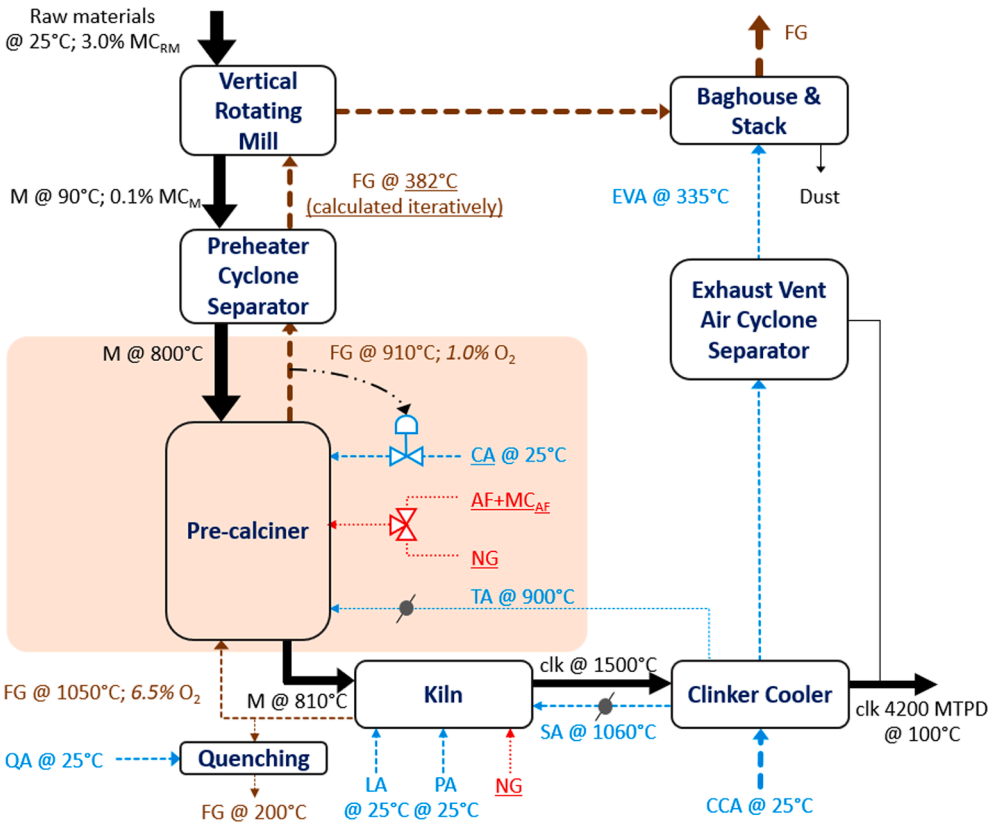

Fig. 1. Process layout of clinker-making technology of a cement plant. **Note: AF - Alternative fuel; CA - Conveying air; CCA - Clinker cooler air; EVA - Exhaust vent air; FG - Flue gas; LA - Leak air; M - Materials; MC - Moisture content; NG - Natural gas; PA - Primary air; QA - Quenching air; RM - Raw materials; SA - Secondary air; TA - Tertiary air. All shown numbers are plant-specific data. The italic numbers are input variables (plant-specific data points) and the underlined numbers are calculated values. (Solid line – Solid flow; Dash line – Gas (Flue gas – Dark brown and Air - Light blue) flow; Dot line – Fuel flow).** (For interpretation of the references to colour in this figure legend, the reader is referred to the web version of this article.)

this study investigated for the AF co-firing. In all co-firing cases, all temperatures except the temperature of the flue gas at the exit of the preheater (underlined values in Fig. 1) were assumed to be similar to that of the reference case cement plant with 100% NG combustion.

2.3. Thermal energy flow model

A thermal energy flow (TEF) model was built for the cement plant depicted in Fig. 1. The process flow diagram including all materials flowing in and out from different components used for modeling the clinker-making process is shown in **Figure S1** in the supplementary file.

2.3.1. Raw material and chemical reactions in the pre-calciner and kiln

Raw materials were supplied by mixing sandstone, black shale, red shale, mill scale, and limestone so that the mixture could provide enough oxides of calcium (CaO), aluminium (Al_2O_3), silicon (SiO_2) and iron (Fe_2O_3) necessary to form clinker. The plant-specific mineral compositions of respective sources of the raw materials and the clinker are presented in **Table S1**. As this study aims to examine the effect of using AFs in the pre-calciner, the composition of clinker, hence the proportion of raw materials mix, was kept constant. Premixed raw materials are milled and dried before it is fed into the pre-heater tower. Typically, the pre-calciner requires a temperature range of 700–950 °C [24] and 1450–2000 °C in the rotary kiln [11,13,25,26] to establish calcining and sintering reactions, respectively.

This study assumed no chemical decompositions reactions in the preheater tower [27] and incorporated 6 chemical reactions in the pre-calciner and rotary kiln as presented in Table A.1 in **Appendix A**. The enthalpies of the calcining and sintering reactions were estimated using the standard heat of formation of the molecules in the chemical reactions. The standard heat of the formation of different molecules is provided in **Table S2**.

2.3.2. Fuel combustion

As shown in Fig. 1, fuels are burned using secondary and primary air in the rotary kiln and using tertiary air in the pre-calciner to support the thermal energy needed in the clinker-making process. The rotary kiln brings in enough air to ensure that 6.5% [O_2] in the kiln flue gas passes on to the pre-calciner, and the pre-calciner brings in enough air to ensure complete combustion of fuel, leaving the flue gas [O_2] 1% or higher. To estimate the fuel and air demands and to predict the amount of flue gas and its composition, the stoichiometric combustion analysis and an actual combustion analysis in the rotary kiln and pre-calciner were established. They are summarized in **Appendix B**. The developed TEF model allows to assess AF co-firing with NG both in the rotary kiln and pre-calciner, but this study has examined only the case of AF co-firing in the pre-calciner.

2.3.3. Mass and energy balances

Fig. 2 explains the mass and energy balances in the pre-calciner and rotary kiln that were established to estimate the fuel demand in the clinker-making process. The derived expressions are presented in **Appendix C.** As can be seen from Fig. 2, the amount of fuel (NG or NG and AF) and the flue gas flowrate are interrelated, therefore an iterative approach was used to determine the fuel demand needed to achieve the set process temperature of the clinker-making process. A detailed mass and energy balances of all the remaining components of the clinker-making process is presented in **Section 5** of the supplementary file.

2.3.4. Specific heat capacity of gases and solids

Since the clinker-making process involves a wide range of temperature, the sensible heat of flue gas and solid materials entering in and leaving out from each component was estimated by using the temperature-dependent expressions for the specific heat capacity. As described in **Appendix D**, the temperature-dependent Shomate

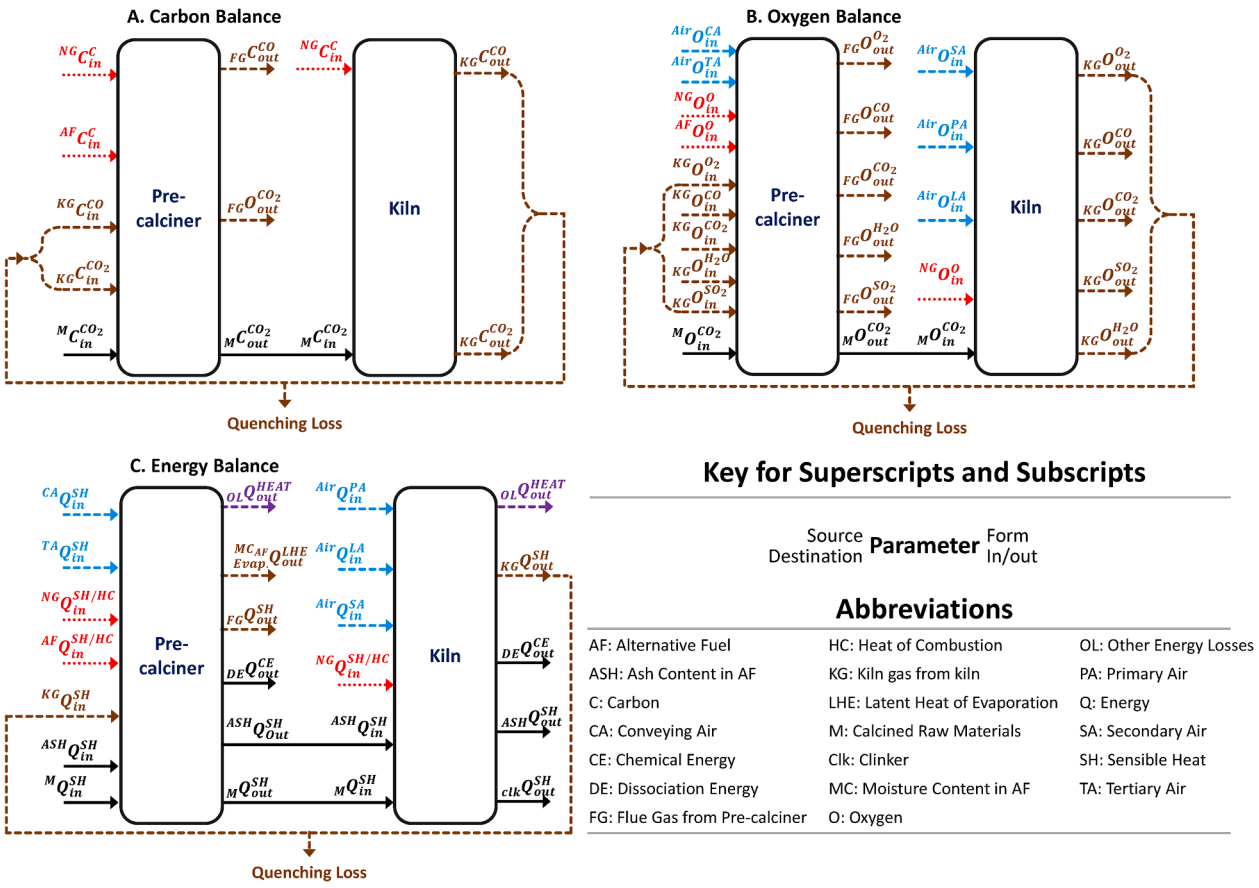

Fig. 2. Steady state flow balance in pre-calciner and kiln: A) Carbon ($^{Source}_{Destination}C^{Form}_{on/out}$); B) Oxygen ($^{Source}_{Destination}O^{Form}_{on/out}$); and C) Energy ($^{Source}_{Destination}Q^{Form}_{on/out}$), where fuel supply is depicted as red, air supply as blue, flue gases as brown, solid materials as black, and heat losses as purple. (For interpretation of the references to colour in this figure legend, the reader is referred to the web version of this article.)

equation [28] was used to determine the specific heat capacity of gases in the flue gas. To estimate the specific heat capacities of the major components of raw materials and clinkers such as SiO_2, Al_2O_3, Fe_2O_3, $CaCO_3$, $MgCO_3$, CaO, MgO, tricalcium silicate (Alite-C_3S), dicalcium silicate (Belite-C_2S), tricalcium aluminate (C_3A) and tetracalcium aluminoferrite (C_4AF), the temperature-dependent functions were used [29–31]. The temperature-dependent correlations of specific heat capacity of solid components are presented in **Table S4** in the supplementary file.

2.3.5. *Case study and model assumptions*

The developed TEF model represented a layout of a dry clinker-making process plant of capacity 4200 tonnes per day. The plant has a 4-stage cyclone preheater system followed by a long cylindrical vertical pre-calciner that completes the majority of the calcining reactions. The calcined raw materials move along with the flue gas from the pre-calciner through a bottom cyclone separator (Cy: V, see **Figure S1**) and then enter into the rotary kiln. The plant uses natural gas as a baseline fuel in the pre-calciner and rotary kiln. In addition, the following assumptions were made:

- Since AF co-firing could impact other aspects such as environmental performance (air pollutants level), impact on traffic due to AF transport and health issues of burning AF, their studies [32] have been carried out separately and therefore were not considered here. In addition, due to the design flexibility of the cement plant, the impact of AF co-firing on the clinker production rate and operational issues were also excluded from this study.
- The changes in electrical power demand that is needed to handle the additional air demand and flue gas flow are important in the cost analysis and life cycle GHG emissions, but it does not affect the overall thermal process of clinker-making. Therefore, the estimation of electrical power demand was not part of the TEF model.
- Materials flows were steady-state and gases were ideal.
- In the reference case, 60% of GJ supplied was in the pre-calciner and the rest in the rotary kiln.
- This study, because it examined the case when 50% of GJ demand in the pre-calciner was to be substituted by AFs, used $\theta_{AF-PC} = 0.5$.
- Any air leakages except in the kiln (3% of the air supply) were neglected.
- The solid collection efficiency of cyclone separators (Cy: II to Cy: V, Cy: EVA) was 95% except for Cy: I = 98% (refer **Figure S1**).
- While the dust leaving kilns were neglected, the dust leaving the preheater tower was estimated using the efficiency of the cyclone separators.
- Clinker dust leaving exhaust vent air cyclone was 1% of clinker production.
- The temperature of the flue gas and the entrained solids leaving together from the pre-calciner and the cyclone separators are in thermal equilibrium.
- Since natural gas-fired cement plants tend to produce 26%-54% more NOx than a coal-fired cement plant [33], the facility studied here was equipped with a Low NOx Calciner Burner and selective non-catalytic reduction [34]. Therefore, this study excluded a detailed analysis of NOx formation.
- The ash (non-combustible material) content in AFs was incorporated in the calculation of the energy and material flows in the TEF model,

but the impact of mineral compositions of the ash on the clinker quality was not included.
- The developed model assumed there will not be unburn carbon if AF is co-fired in the rotary kiln, but there may be unburned char in the pre-calciner. This study, however, assumed that AF burned completely without leaving any unburned char in the pre-calciner ($m_9 = 0 \quad in \quad Eq.(B.3); C_{UB-C-K-i} = 0 \quad in \quad Eq.(B.2)$).

The TEF model results for the reference case was validated using the plant-specific data for the process temperatures, and materials and gases flow into and out of the kiln, pre-calciner and clinker cooler. The model assumptions and projections were within ±5% of the plant-specific data which are not presented here for reasons of confidentiality. The validated TEF model was then used to predict the changes in the air, energy, and emissions intensities when AFs were co-fired to replace 50% of GJ demand in the pre-calciner. Table 2 presents all plant-specific input variables and calculated parameters for the reference case and other examined cases (1 to 4):

- Reference case: NG as a fuel keeping 1% [O_2] in the flue gas at the exit of pre-calciner – [NG-1]
- Case 1 (To examine the effect of AF co-firing without incorporating the effect of [O_2] in the flue gas): AFs (dry basis) replaced 50% of pre-calciner GJ demand keeping 1% [O_2] in the flue gas at the exit of the pre-calciner – [NG/AF-1].
- Case 2 (To examine the effect of AF co-firing by incorporating the effect of [O_2] in the flue gas): AFs (dry basis) replaced 50% of pre-calciner GJ demand keeping 3% [O_2] in the flue gas at the exit of pre-calciner – [NG/AF-3]
- Case 3 (To examine the effect of the moisture content in AFs): Keeping 1% [O_2] in the flue gas at the exit of the pre-calciner, 50% of pre-calciner GJ demand was substituted by AFs with the moisture content (MC) of 10%; 15%, and 20%.
- Case 4 (To examine the effect of the [O_2] in the flue gas): 50% of GJ demand in pre-calciner was substituted by AFs (dry basis) by changing [O_2] in the flue gas at the exit of pre-calciner to 3%, 5% and 6% [O_2]. Repeat Case 3 at each of these new oxygen concentrations in the flue gas.

The CO concentration in the flue gas was assumed to be 0.02% (mole basis) for all cases based on the pre-calciner plant design [34]. This is a reasonable assumption for a plant consuming natural gas with 1% [O_2] in the flue gas (Reference Case), or for a co-fired plant where AFs have a very small particle size (Cases 1 and 3). With larger particle sizes for the AFs, a higher flue gas oxygen requirement would be needed to ensure complete combustion and a low CO concentration in the flue gas (Cases 2 and 4).

Table 2
Reference Case information and summary of examined variables.

Parameters	Reference case	Examined range
Input variable		
[O_2] in flue gas at kiln exit, % mole	6.5	Kept constant
[O_2] in flue gas at pre-calciner exit, % mole	1.0	1.0 to 6.0
[CO] in flue gas, % mole	0.02	Kept constant
Share of AF in pre-calciner, % GJ basis	100	50
Share of AF in kiln, % GJ basis	0.0	0.0
Moisture in alternative fuels, % wt.	0.0	0.0 to 20.0
LHV and elemental compositions of AF, dry basis	N/A	See Table 1
Calculated parameter		
Air demand, Nm^3/t clk	• TBD	• TBD
Thermal energy intensity, MJ/t clk	• TBD	• TBD
Fuel-related combustion emissions, tCO_2/t clk	• TBD	• TBD

2.4. Generalized regression equations

Using the results of the energy demands of clinker-making for 24 AFs and NG predicted by the TEF model (Results of reference case and case 1), regression equations were developed for thermal energy intensity (TEI, MJ/t clk) using lower heating value (LHV) and embedded elemental oxygen fraction (O) of fuel.

Since a linear regression equation did not provide a good fit to the TEF modeled data, resulting in a higher mean absolute error (MAE) than the non-linear curve fit, a second-order curve fit was developed as shown in **Eq. (1)**:

$$TEI_{MC=0,[O_2]=1\%} = c_1 + c_2 \times (LHV) + c_3 \times (O) + c_4 \times (LHV) \times (O) + c_5 \times (LHV)^2 + c_6 \times (O)^2 \quad (1)$$

where, $TEI_{MC=0,[O_2]=1\%}$ is the thermal energy intensity when an AF was co-fired at the dried condition (Moisture content of 0%) with 1% [O_2] in the flue gas at the pre-calciner exit. The values of constants $c_1 \quad to \quad c_6$ were determined by minimizing the sum of square error method using the Solver tool in Microsoft Excel in Office 365, version 2019.

Similarly, to predict the changes in the TEI with the moisture content (MC) (>0%) in AFs and the [O_2] in flue gas (>1%) at the exit of the pre-calciner, more TEF model results generated in cases 3 and 4 were used to devise both linear (ignoring constant terms c_8, and c_{10}) and non-linear equations of MC and [O_2] as shown in **Eq. (1a)**. The regression equation with a lower MAE value was then selected:

$$TEI = TEI_{MC=0,[O_2]=1\%} + \{c_7 + c_8 \times (MC)\} \times (MC) + \{c_9 + c_{10} \times ([O_2]-1)\} \times ([O_2]-1) \quad (1a)$$

3. Result and discussions

3.1. Reference case (NG-1)

The new cement plant (Lafargeholcim Exshaw plant retrofitted in 2018) in this study has several features that enhance thermal efficiency, including multi-stage preheating, a separate pre-calciner and kiln, and the ability to use natural gas making it possible to achieve complete combustion with a flue gas [O_2] as low as 1%. Under these conditions, the thermal energy flow (TEF) model was developed to assess the performance of its clinker-making process. Table 3 presents a summary of thermal energy and material flows predicted by the TEF model. The TEF model results for the reference case presented in Table 3 and the flue gas composition summarized in **Table S5** (at the exit of the rotary kiln and pre-calciner) was in close agreement with the plant-specific data. A summary of air supply and excess air in the rotary kiln, the pre-calciner, and the overall clinker-making process is also presented in **Table S6** of the supplementary file.

The clinker-making process requires 1.58 kg of raw materials (dry) for each kg of clinker (clk), resulting in process emissions of 556 $kgCO_2$/t clk (Table 3, **R24**), a value that is similar to previous reports [35–37].

The TEF model estimates thermal energy intensity (TEI) of 3293 MJ_{LHV}/t clk (Table 3, **R1**) of which 60% is supplied to the pre-calciner and the remaining to the rotary kiln. This TEI is lower than the average energy intensity of 4500 MJ_{LHV}/t clk for other cement plants in Canada [38]. Of the total thermal energy supplied, 53% (1737 MJ/t clk) supports the calcining and sintering reactions listed in Table A.1, a value that is similar to those reported in other studies [26,39–42]. The flue gas losses (FGL) of 17.7% (Table 3, **R26**) and exhaust vent air losses (EVAL) of 7.9% (Table 3, **R27**) are also within the reported literature values [42].

The TEF model also estimates that primary air (PA) supply of 34 Nm^3/t clk (Table 3, **R10**) is supplemented by secondary air (SA) at 512 Nm^3/t clk (Table 3, **R11**) reflecting the need to support combustion and maintain 6.5% [O_2] in flue gas at the kiln exit. This excess oxygen enters

Table 3
Results of the TEF model: Co-firing AF in pre-calciner keeping 1% [O_2] in flue gas at the exit of pre-calciner (Case: 1).

Row	Results	Units	Ref.	AF at 50% of pre-calciner's energy demand with 50% NG																							
			[NG:1]	RC	HDPE	TVBP	EPW1	CG	EPW2	SC	AS	WT	SOC	BIW	CH	SW	WD	BM	RT1	PW	TP	RT2	LW	CB	PO	T	P
R1	**A. Thermal Energy Intensity (TEI)**	GJ_{LHV}/t clk	3.293	3.277	**3.272**	3.264	3.275	3.302	3.286	3.291	3.336	3.274	3.331	3.310	3.312	3.319	**3.323**	3.326	3.304	3.310	3.305	**3.305**	3.299	3.334	3.330	3.355	3.335
R2	NG in Kiln		1.311	1.314	**1.311**	1.311	1.313	1.316	1.316	1.311	1.334	1.311	1.314	1.312	1.312	1.315	**1.319**	1.317	1.311	1.312	1.312	**1.311**	1.311	1.315	1.313	1.311	1.312
R3	NG in PC		1.982	0.982	**0.981**	0.976	0.981	0.992	0.985	0.990	1.001	0.981	1.008	0.998	1.000	1.002	**1.002**	1.004	0.996	0.999	0.997	**0.997**	0.994	1.009	1.008	1.022	1.011
R4	AF in PC		0.000	0.982	**0.981**	0.976	0.981	0.992	0.985	0.990	1.001	0.981	1.008	0.998	1.000	1.002	**1.002**	1.004	0.996	0.999	0.997	**0.997**	0.994	1.009	1.008	1.022	1.011
R5	Total energy demand	GJ_{LHV}/hr	576	573	**573**	571	573	578	575	576	584	573	583	579	579	581	**582**	582	578	579	578	**578**	577	583	583	587	584
R6	NG in Kiln	tonne of fuel/t clk	4.84	4.85	**4.84**	4.84	4.85	4.86	4.86	4.84	4.92	4.84	4.85	4.84	4.84	4.85	**4.87**	4.86	4.84	4.84	4.84	**4.84**	4.84	4.85	4.85	4.84	4.84
R7	NG in PC		7.32	3.63	**3.62**	3.60	3.62	3.66	3.64	3.66	3.70	3.62	3.72	3.69	3.69	3.70	**3.70**	3.71	3.68	3.69	3.68	**3.68**	3.67	3.73	3.72	3.77	3.73
R8	AF in PC		0.00	4.80	**3.98**	4.54	5.61	8.57	6.88	6.88	13.04	5.24	11.51	8.67	9.34	10.26	**10.96**	9.65	8.86	9.53	8.61	**8.59**	7.95	11.52	11.38	12.78	11.17
R9	**B. Air Demand (AD)**	Nm^3/t clk	1591	1691	**1649**	1686	1677	1721	1666	1679	1740	1609	1675	1618	1648	1652	**1651**	1510	1649	1656	1609	**1609**	1590	1601	1611	1559	1531
R10	Primary air		34	34	**34**	34	34	34	34	34	34	34	34	34	34	34	**34**	34	34	34	34	**34**	34	34	34	34	34
R11	Secondary air		512	513	**512**	512	513	514	514	512	521	512	513	513	512	514	**515**	515	512	512	512	**512**	512	514	513	512	512
R12	Leak air kiln		16	16	**16**	16	16	16	16	16	17	16	16	16	16	16	**16**	16	16	16	16	**16**	16	16	16	16	16
R13	Tertiary air		430	386	**403**	385	392	375	401	388	385	422	394	419	404	406	**411**	476	403	400	423	**422**	431	430	424	446	460
R14	Exhaust vent air		614	758	**700**	754	738	798	717	745	800	641	733	651	696	698	**691**	485	699	709	639	**641**	612	622	640	566	525
R15	Total combustion air (TCA)		993	950	**965**	948	956	940	966	951	957	984	958	983	968	970	**977**	1041	966	963	986	**985**	994	995	987	1009	1023
R16	**C. Emissions Intensity (EI)**	$kgCO_2$/t clk	744	753	**758**	765	766	769	769	769	776	777	782	780	784	786	**787**	788	787	787	788	**789**	791	796	797	799	804
R17	EI excluding Bio. C		744	753	**758**	765	766	769	769	687	758	777	689	688	688	688	**689**	689	714	736	735	**714**	688	689	689	689	742
R18	Energy emissions include Bio. C		188	197	**203**	209	210	213	213	213	220	222	226	225	229	230	**231**	232	231	231	232	**233**	235	240	241	243	248
R19	AF emissions-PC		0	66	**71**	78	79	81	81	82	86	91	93	92	96	97	**99**	99	99	99	100	**101**	103	107	108	110	116
R20	Fossil C		0	66	**71**	78	79	81	81	0	69	91	0	0	0	0	**0**	0	26	48	47	**26**	0	0	0	0	53
R21	Biogenic C (Bio.C)		0	0	**0**	0	0	0	0	82	17	0	93	92	96	97	**99**	99	73	52	53	**74**	103	107	108	110	62
R22	NG emissions-PC		113	56	**56**	56	56	57	56	57	57	56	58	57	57	57	**57**	58	57	57	57	**57**	57	58	58	59	58
R23	NG emissions-K		75	75	**75**	75	75	75	75	75	76	75	75	75	75	75	**75**	75	75	75	75	**75**	75	75	75	75	75
R24	Process emissions		556	556	**556**	556	556	556	556	556	556	556	556	556	556	556	**556**	556	556	556	556	**556**	556	556	556	556	556
R25	**D. Waste Heat**	GJ/t clk	0.841	0.826	**0.822**	0.815	0.824	0.850	0.834	0.841	0.877	0.823	0.878	0.857	0.860	0.866	**0.868**	0.869	0.852	0.858	0.853	**0.853**	0.846	0.879	0.876	0.900	0.880
R26	Flue gas loss (FGL)		0.581	0.505	**0.527**	0.496	0.512	0.513	0.531	0.526	0.539	0.552	0.568	0.581	0.565	0.570	**0.576**	0.664	0.557	0.558	0.582	**0.582**	0.588	0.616	0.606	0.660	0.658
R27	Exhaust vent air loss (EVAL)		0.260	0.321	**0.296**	0.319	0.312	0.337	0.303	0.315	0.338	0.271	0.310	0.275	0.294	0.295	**0.292**	0.205	0.295	0.300	0.270	**0.271**	0.259	0.263	0.271	0.239	0.222

the pre-calciner and is supplemented by tertiary air (TA) at 430 Nm^3/t clk (Table 3, **R13**), resulting in a total combustion air requirement of 993 Nm^3/t clk (Table 3, **R15**), including about 16 Nm^3/t clk of leakage into the kiln system, and 1% [O_2] in the flue gas. In addition, there is an exhaust vent air demand of 614 Nm^3/t clk (Table 3, **R14**) to cool the clinker, resulting in a thermal energy loss of 7.9% (260 MJ/t clk) of the total TEI.

The CO_2 emission intensity depends mainly on direct emissions due to fuel combustion and limestone decompositions, and indirect emission from electricity consumption. As this study focuses mainly on the thermal energy requirement, details of indirect CO_2 emissions due to electricity consumption are not included here. Henceforth, all emissions in this study will be direct emissions. The combustion of NG in the kiln and pre-calciner produces 75 $kgCO_2$/t clk (Table 3, **R23**) and 113 $kgCO_2$/t clk (Table 3, **R22**), respectively. Therefore, the total CO_2 emissions intensity including process emissions is 744 $kgCO_2$/t clk (Table 3, **R16**).

3.2. Alternative fuel scenarios: [NG/AF-1] and [NG/AF-3]

The TEF model was used to explore the use of solid AFs to replace 50% of the fuel energy input to the pre-calciner where natural gas provided the balance of pre-calciner energy and all of the kiln energy demands. While 24 AFs were studied and compared to the natural gas reference case , three of the AFs (Bolded rows in Table 1) were selected for their diversity in biogenic carbon content for a more detailed assessment. They were:

- HDPE: High-density polythene (no biogenic carbon)
- WD: Wood dust (100% biogenic carbon)
- RT2: Railway ties (74% biogenic carbon)

Typically, complete combustion of solid fuels is not possible without providing excess air supply that ultimately results in flue gas oxygen

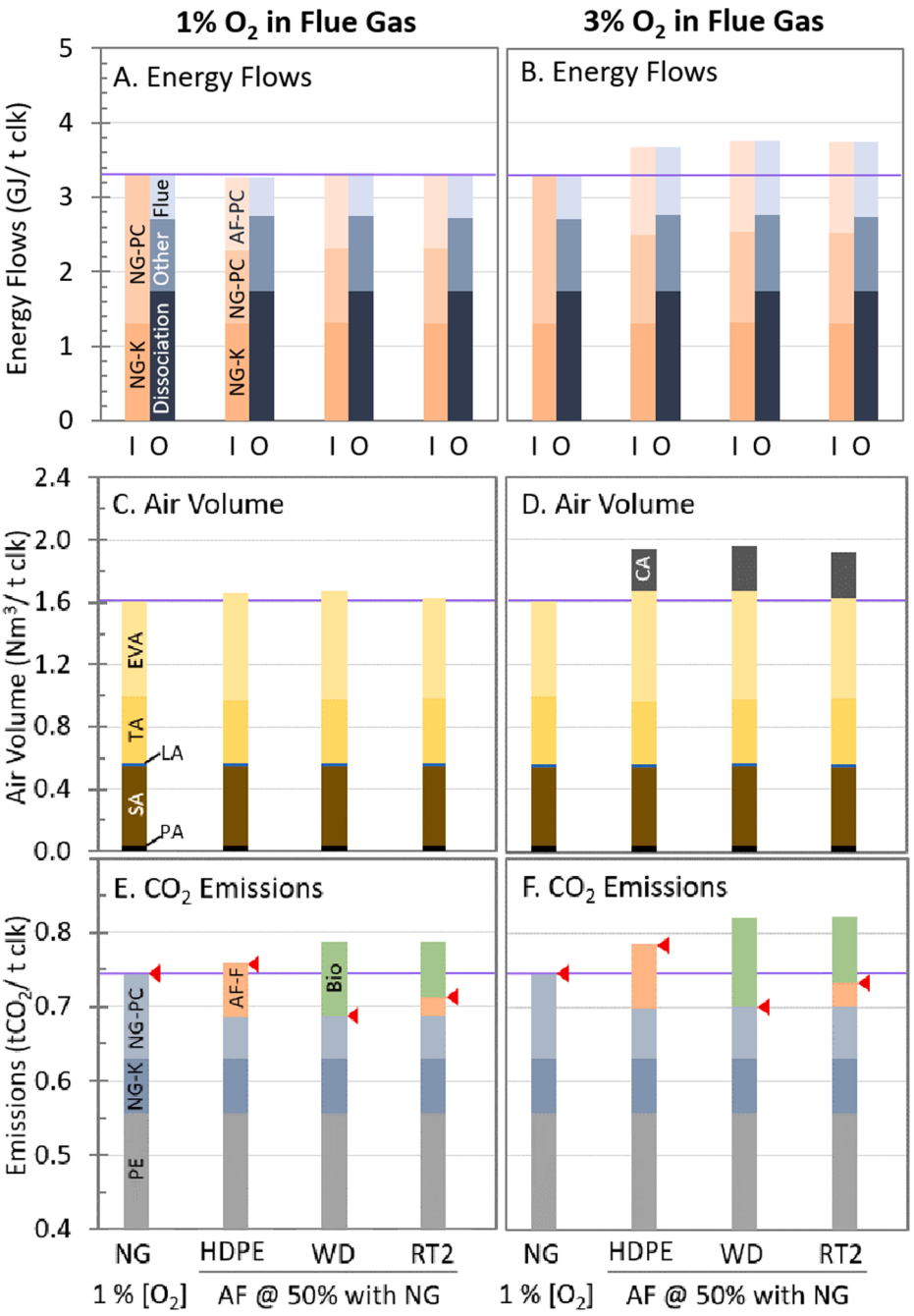

Fig. 3. Effects of AF co-firing at 1% and 3% [O_2] in flue gas on energy flows (I-In & O-Out), air demand and CO_2 emissions. Note that both natural gas (NG) only cases had a flue gas [O_2] of 1%. (Note: AF-F: Fossil emissions from AF; AF-PC: AF energy input in PC; Bio: Biogenic emissions; CA: Conveying air; Dissociation: Dissociation energy input to breakdown limestone; EE: Energy Emissions; EVA: Exhaust vent air; Flue: Flue gas loss; HDPE: Plastic Waste; LA: Leak air; NG-K: NG input in kiln and its emissions; NG-PC: NG input in PC and its emissions; PA: Primary air; PE: Process Emissions; Other: Other losses that includes exhaust vent air loss, radiation and unaccounted losses; RT2: Railway Ties 2; SA: Secondary air; TA: Tertiary air; WD: Wood dust; represents the net GHG emissions; $GWP_{Bio} = 0$).

concentrations of 2% to 7% or more [15]. To explore the importance of oxygen concentration in the flue gas [O_2] on the energy and material flows through the clinker-making process, scenarios assuming both 1% and 3% in the flue gas were carried out with the TEF model and their summary for the selected AFs are shown in Fig. 3.

1% [O_2] in Flue Gas (Case 1). The flows of energy, air, and CO_2 for 24 AFs and reference natural gas fuels are presented in Table 3. Compared to the reference case, the TEI of the clinker-making process decreased by 0.6% for HDPE and increased by 0.9% for WD and 0.4% for RT2 when the respective AFs were co-fired (Fig. 3**A**). The decrease in TEI with HDPE (assuming complete combustion of the HDPE can be achieved when there is only 1% [O_2] in the flue gas) is due to a reduction in the total combustion air (TCA) supply from 993 Nm^3/t clk to 965 Nm^3/t clk (Table 3, **R15**), thereby avoiding the need to heat the air to process temperatures. The decreased in TCA supply could be explained, in part, by the higher level of embedded elemental oxygen content in the HDPE compared to that in NG (0.9% vs 0%, Table 1).

Similar results for TCA are also observed for woody biomass fuels such as WD and RT2, which have significantly higher embedded elemental oxygen content in the range of 32–36% (Table 1). However, the TEI for WD and RT2 is higher than the reference case since TEI not only depends on embedded elemental oxygen content in the AFs but also on its lower heating value (LHV) and moisture content. If the LHV of the AF was low, more fuel (Table 3, **R7 and R8**) would have to be combusted to supplement the increase in sensible heat demand and heat of evaporation of the moisture in the AF. For example, the WD with low LHV of 16.1 MJ_{LHV}/kg resulted in higher TEI compared to the RT2 with LHV of 20.4 MJ_{LHV}/kg (Table 3, **R1**).

Since the tertiary air (TA) demand supplying to the pre-calciner is drawn from the clinker cooler exhaust, a reduction in that air demand for three selected AFs results in an increase in the exhaust vent air by 14%, 12% and 4% for HDPE, WD, and RT2, respectively. This, therefore, increases the respective total air demand (AD) by 3.6%, 3.8%, and 1.2% (Table 3, **R9**) as shown in Fig. 3**C**.

Due to the higher carbon intensity of AFs compared to NG (Table 1), all AFs co-firing have higher total emissions intensity ($kgCO_2$/t clk), ranging from 1.2 to 8.1% (Table 3, **R16**). However, not all carbon in the AFs are from fossil fuel sources, therefore the total GHG emission intensity using an AF like WD, resulted in a 7.5% reduction (56 $kgCO_2$/t clk) compared to the NG-based reference plant (Table 3, **R17,** Fig. 3**E**). By comparison, HDPE (0% biogenic C) increases the total GHG emission intensity by 1.9% (Fig. 3**E**).

As noted previously, complete combustion of AFs can rarely be achieved with a flue gas [O_2] of only 1%. Therefore, the effect of increasing flue gas [O_2] to 3% was modeled and compared to the NG-based reference plant having only 1% [O_2] in the flue gas.

3% [O_2] in Flue Gas for AF only (Case 3). To ensure complete combustion of the AFs, 3% flue gas [O_2] is assumed, made possible by supplying additional air from the conveying air stream to the pre-calciner (Table 4**, R14**). This results in more thermal heat loss from the flue gas stream as shown in Fig. 3**B**. On average, the shift to 3% [O_2] in the AF co-firing cases increases the TEI by 443 MJ/t clk (13% more) compared to the NG-based reference cement plant with 1% [O_2] in the flue gas (Table 4, **R1**).

To co-fire AFs and maintain 3% [O_2] in the flue gas, the clinker-making process requires on average of 334 Nm^3/t clk (21%) more air, compared to the NG-based reference cement plant with 1% [O_2] in the flue gas (Table 4, **R9;** Fig. 3**D).**

The requirement to maintain 3% [O_2] in the flue gas of plants using AFs, also increases total CO_2 emission intensity by on average 69 $kgCO_2$/t clk (9.3% more) compared to the NG-based reference cement plant with 1% [O_2] in the flue gas (Table 4, **R17**). In the case if a carbon–neutral AF such as WD, the total GHG intensity was reduced by 5.8% (43 $kgCO_2$/t clk) compared to the NG-based reference cement plant with 1% O_2 in the flue gas. However, non-biogenic waste-derived fuels like HDPE could increase GHGs by 5.5% (41 $kgCO_2$/t clk) (Fig. 3**F**). The RT2 with 74% biogenic carbon is projected to reduce GHGs by 1.6% (12 $kgCO_2$/t clk) (Fig. 3**F**). Therefore, for AFs lacking biogenic carbon, the cement plant operator would face a trade-off between the cost of AFs and the cost of the excess CO_2 emissions with respect to the emission benchmark.

The GHG values presented here (Fig. 3**E and F**) only consider the direct CO_2 emission for which the cement plant operator is responsible for the carbon price regulation in Canada. In the reference cement plant, these include process emissions of 556 kg CO_2e/t clk and fuel combusted related emissions of 188 kg CO_2e/t clk. Life cycle emissions would be higher and include:

- Upstream emissions associated with the production and pipeline distribution of NG are estimated to be 18% more compared to its carbon intensity [43]. Therefore, for the reference plant, including life cycle emissions would increase energy emissions by about 34 CO_2e/t clk.
- For the cement plants using AFs, additional emissions may be associated with the processing and delivery of AFs, but not with their production processes since they are all from waste streams. On the other hand, there may be emission reductions resulting from the diversion of biomass from landfill sites where methane can be released due to anaerobic digestion [10].
- Indirect CO_2 emissions associated with electricity use (about 90 kwh/t clk for the reference clinker-making process) would add 61 $kgCO_2$e/t clk, given the emission intensity of the grid in Alberta, Canada of 680 kg CO_2/MWh [44].
- Due to the increase in air demand and the flue gas volume for plants using AF, electricity demand is expected to increase by about 14 kWh/t clk (16%) over the 90 kWh/t clk in the reference case. This would result in an additional 10 $kgCO_2$e/t clk of indirect emissions.

The Effect of AF on Flue Gas Composition and Flow. Compared to the reference case plant with 1% [O_2], the AFs cases at 3% [O_2] in the flue gas show an increase in the flue gas volumetric flow (15 to 29%), and thermal flue gas loss (49 to 97%) (**Table S7)**. This is primarily due to the need for excess air when AFs are combusted.

Even though CO_2 emissions per tonne clinker are higher when AFs are combusted, the increased volumetric flow of the flue gas results in the concentration of CO_2 being reduced from about 27% CO_2 in the reference case to 23 to 25% CO_2 in the AF cases. However, the thermal flue gas loss from CO_2 increases from 0.20 GJ/t clk in the reference case to 0.29 to 0.36 GJ/t clk in the AF cases.

3.3. Regression for thermal energy intensity (TEI)

The results of the TEF model (Tables 3 and 4) identified four major factors that determine the TEI of the clinker-making process, including the embedded elemental oxygen content (O) and lower heating value (LHV) of AFs, as well as required [O_2] in flue gas, and the moisture content (MC) of AFs. To examine the combined effect of these parameters on the TEI and provide a quick assessment of the performance of clinker-making under AF co-firing cases, a regression equation was developed here. The TEF model results in Tables 3 and 4 along with the results obtained for cases 3 and 4 were used to generate the regression equation making it possible to calculate TEI for a wide range of AFs without needing to run the full TEF model for the cement plant:

$$TEI = 3488.5 - 11.5 \times (LHV) - 182.6 \times (O) + 3.2 \times (LHV) \times (O) + 15.4 \times 10^{-2} \times (LHV)^2 + 232.0 \times (O)^2 + 3.1 \times (MC) + \{42.4 \times ([O_2] - 1) + 131.2\} \times ([O_2] - 1) \quad (2)$$

As shown in Fig. 4, this regression equation provides a good fit to the TEF-modeled TEI for the 24 AFs with known values for embedded elemental oxygen content (O) and LHV. The mean absolute error (MAE)

Table 4
Results of the TEF model: Co-firing AF in pre-calciner keeping 3% [O_2] in flue gas at the exit of pre-calciner (Case: 2).

Row	Results	Unit	Ref. [NG:1]	[NG:3]	AF at 50% of pre-calciner's energy demand with 50% NG																							
					RC	HDPE	TVBP	EPW1	CG	EPW2	SC	AS	WT	SOC	BIW	CH	SW	WD	BM	RT1	PW	TP	RT2	LW	CB	PO	T	P
R1	**A. Thermal Energy Intensity (TEI)**	GJ_{LHV}/t clk	3.293	3.735	3.669	**3.678**	3.650	3.671	3.693	3.693	3.691	3.746	3.697	3.752	3.746	3.734	3.745	**3.755**	3.830	3.722	3.727	3.742	**3.742**	3.742	3.791	3.779	3.839	3.825
R2	NG in Kiln		1.311	1.311	1.314	**1.311**	1.311	1.314	1.318	1.317	1.311	1.338	1.311	1.315	1.313	1.312	1.316	**1.321**	1.318	1.311	1.312	1.312	**1.311**	1.311	1.316	1.314	1.311	1.312
R3	NG in PC		1.982	2.424	1.177	**1.184**	1.169	1.179	1.188	1.188	1.190	1.204	1.193	1.219	1.216	1.211	1.214	**1.217**	1.256	1.205	1.208	1.215	**1.215**	1.215	1.237	1.232	1.264	1.256
R4	AF in PC		0.000	0.000	1.177	**1.184**	1.169	1.179	1.188	1.188	1.190	1.204	1.193	1.219	1.216	1.211	1.214	**1.217**	1.256	1.205	1.208	1.215	**1.215**	1.215	1.237	1.232	1.264	1.256
R5	Total energy demand	GJ_{LHV}/hr	576	654	642	**644**	639	642	646	646	646	655	647	657	655	653	655	**657**	670	651	652	655	**655**	655	663	661	672	669
R6	NG in Kiln	tonne of fuel/t	4.838	4.838	4.850	**4.838**	4.839	4.849	4.863	4.862	4.838	4.939	4.838	4.852	4.845	4.842	4.855	**4.875**	4.866	4.839	4.841	4.842	**4.840**	4.839	4.856	4.849	4.838	4.842
R7	NG in PC	clk	7.32	8.96	4.35	**4.37**	4.32	4.35	4.38	4.39	4.39	4.44	4.40	4.50	4.49	4.47	4.48	**4.49**	4.64	4.45	4.46	4.49	**4.48**	4.48	4.57	4.55	4.66	4.64
R8	AF in PC		0.00	0.00	5.76	**4.80**	5.44	6.74	10.25	8.30	8.27	15.68	6.37	13.92	10.56	11.31	12.44	**13.31**	12.07	10.72	11.52	10.49	**10.48**	9.72	14.12	13.91	15.81	13.88
R9	**B. Air Demand (AD)**	Nm^3/t clk	1591	1890	1959	**1925**	1950	1948	1986	1944	1949	2021	1897	1955	1911	1930	1937	**1942**	1849	1929	1936	1902	**1903**	1888	1905	1909	1876	1856
R10	Primary air		34	34	34	**34**	34	34	34	34	34	34	34	34	34	34	34	**34**	34	34	34	34	**34**	34	34	34	34	34
R11	Secondary air		512	512	513	**512**	512	513	515	515	512	523	512	514	513	513	514	**516**	515	512	512	512	**512**	512	514	513	512	512
R12	Leak air kiln		16	16	16	**16**	16	16	16	16	16	17	16	16	16	16	16	**17**	16	16	16	16	**16**	16	16	16	16	16
R13	Tertiary air		430	430	386	**403**	385	392	375	401	388	385	422	394	419	404	406	**411**	476	403	400	423	**422**	431	430	424	446	460
R14	Conveying air		0	298	266	**277**	264	270	263	276	270	270	288	279	292	282	284	**287**	335	280	279	293	**293**	298	302	297	317	324
R15	Exhaust vent air		614	614	759	**700**	754	739	800	719	745	809	641	734	652	697	700	**694**	488	699	710	640	**641**	612	624	641	566	525
R16	Total combustion air (TCA)		993	1292	1216	**1242**	1213	1226	1203	1242	1221	1229	1273	1237	1275	1250	1254	**1265**	1377	1247	1243	1279	**1278**	1292	1297	1285	1326	1347
R17	**C. Emissions Intensity (EI)**	$kgCO_2$/t clk	744	769	777	**785**	791	793	796	797	797	805	809	813	813	817	819	**821**	827	820	820	822	**823**	826	833	834	839	846
R18	EI excluding Bio. C		744	769	777	**785**	791	793	796	797	699	784	809	701	701	700	701	**701**	703	731	758	758	**732**	700	702	701	703	769
R19	Energy emissions include Bio. C		188	214	222	**229**	235	237	240	241	241	249	253	258	257	261	263	**265**	271	264	264	266	**267**	271	277	278	283	290
R20	AF emissions-PC		0	0	79	**86**	93	95	96	98	98	104	110	113	113	117	118	**120**	124	120	120	122	**123**	126	131	132	136	144
R21	Fossil C		0	0	79	**86**	93	95	96	98	0	83	110	0	0	0	0	**0**	0	31	58	57	**32**	0	0	0	0	66
R22	Biogenic C (Bio.C)		0	0	0	**0**	0	0	0	0	98	21	0	113	113	117	118	**120**	124	89	62	65	**91**	126	131	132	136	77
R23	NG emissions-PC		113	139	67	**68**	67	68	68	68	68	69	68	70	70	69	70	**70**	72	69	69	70	**70**	70	71	71	72	72
R24	NG emissions-K		75	75	75	**75**	75	75	75	75	75	76	75	75	75	75	75	**75**	75	75	75	75	**75**	75	75	75	75	75
R25	Process emissions		556	556	556	**556**	556	556	556	556	556	556	556	556	556	556	556	**556**	556	556	556	556	**556**	556	556	556	556	556
R26	**D. Waste Heat**	GJ/t clk	0.841	1.266	1.203	**1.212**	1.183	1.204	1.225	1.224	1.224	1.269	1.229	1.282	1.276	1.265	1.274	**1.282**	1.354	1.253	1.259	1.273	**1.272**	1.276	1.318	1.307	1.365	1.351
R27	Flue gas loss (FGL)		0.581	1.006	0.882	**0.916**	0.864	0.892	0.887	0.920	0.910	0.927	0.958	0.971	1.000	0.971	0.979	**0.989**	1.147	0.958	0.959	1.002	**1.001**	1.013	1.054	1.036	1.126	1.129
R28	Exhaust vent air loss (EVAL)		0.260	0.260	0.321	**0.296**	0.319	0.312	0.338	0.304	0.315	0.342	0.271	0.310	0.276	0.295	0.296	**0.293**	0.207	0.296	0.300	0.270	**0.271**	0.263	0.264	0.271	0.239	0.222

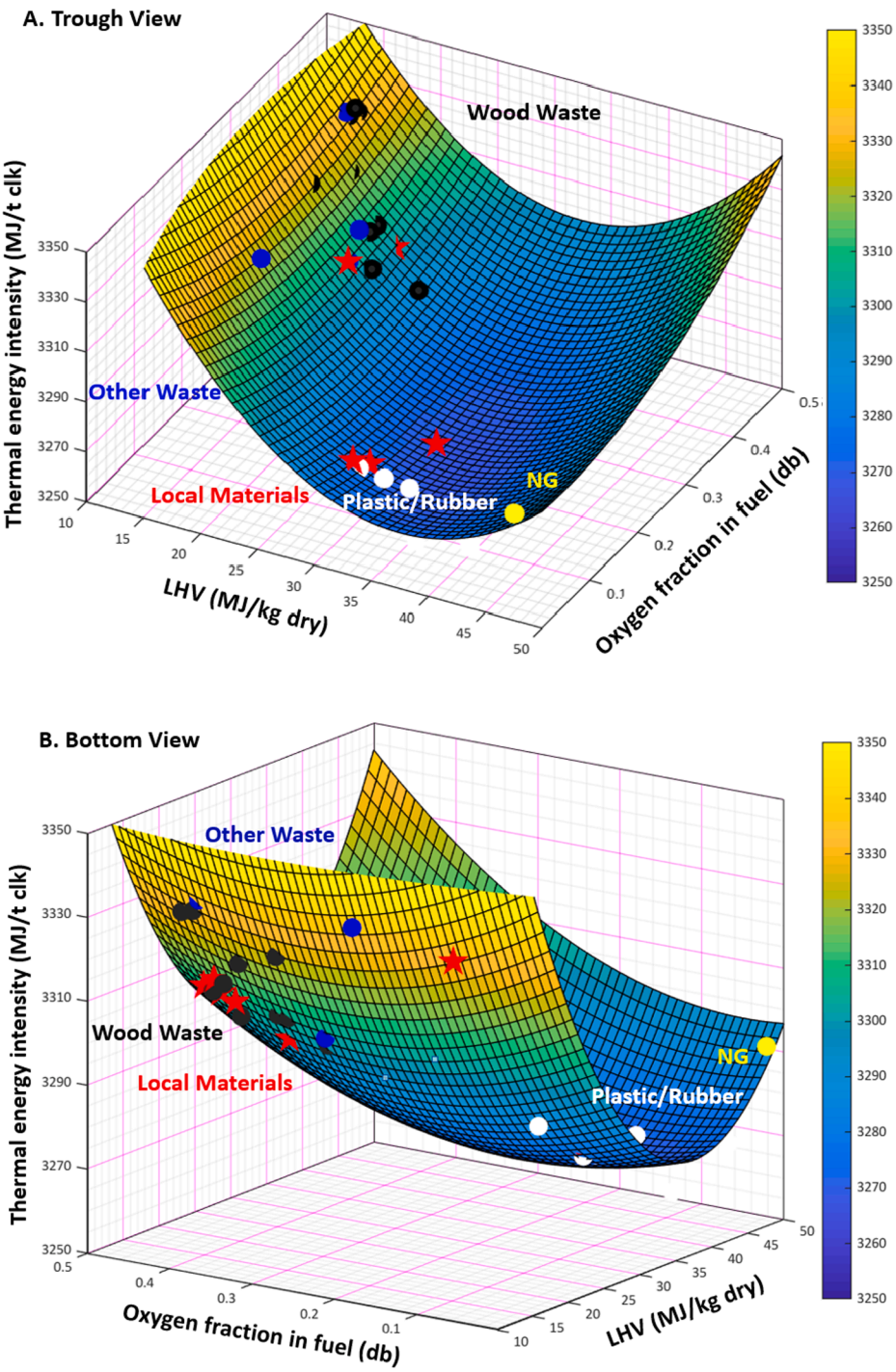

Fig. 4. A curve describing the effect of LHV and embedded elemental oxygen fraction of alternative fuel on the modeled specific thermal energy demand in MJ/t clk (MC in AFs = 0%, $[O_2]$ in pre-calciner exit = 1%; Other waste (blue circle) includes textile, asphalt shingles and carpets; Local materials (red star) include locally available waste-drived alternative fuels); Wood waste (black circle); Plastic/Rubber (white circle); NG (yellow circle)). (For interpretation of the references to colour in this figure legend, the reader is referred to the web version of this article.)

between the TEF modeled TEI and the non-linear curve fit TEI (**Eq. (2)**) is about 5 MJ/t clk, which is less than the MAE of 10 MJ/t clk for the linear regression equation (Refer to **Section S9** and **Table S8** of the supplementary file). To put these numbers in perspective, the range of modeled TEI values with various AFs are within 91 MJ/t clk with the 0% MC and 1% $[O_2]$ in the flue gas data presented in Fig. 4.

The inclusion of non-linear terms of LHV and O also helps to justify the decrease in the TEI for some AFs with high LHV and slightly more embedded elemental oxygen content than that in NG (Refer to the discussion in **Section 3.2**). For other AFs having a lower LHV, the TEI of clinker-making increases thereby forming a concave upward curvature in Fig. 4. It is noted here that this analysis has assumed the same combustion efficiency for AF and NG at the same level of $[O_2]$ in the flue gas.

Validation using Local AF Data. To test the regression equation, embedded elemental oxygen content (O) and LHV values for ten locally available waste-derived AFs are both analyzed by the TEF model to generate values for TEI (red stars in Fig. 4), which were then compared with the TEI value generated by the curve fit (**Eq. (2)**) at 0% MC and 1% $[O_2]$ in the flue gas. The regression equation predicts the TEI for these local fuels within the MAE of 4.4 MJ/t clk (**Table S9**). This supports the premise that **Eq. (2)** can provide a reasonable estimate for the TEI for all wide range of AFs.

Effect of Moisture Content (MC). Most AFs are not completely dry so when they are combusted, the MC of AF would be evaporated, consuming a portion of the supplied fuel energy thereby increasing the TEI required for clinker production. The energy requirement to process

the MC increases linearly with the moisture level as shown in Fig. 5, therefore a simple linear curve fit (as it has similar MAE as that of the non-linear curve fit) was selected in **Eq. (2)**. Note that every 1% increase in the MC in an AF increases the TEI by about 3.1 MJ/t clk. Therefore, in a typical AF with an average 10% MC [45], the TEI increases by 31 MJ/t clk, or approximately a 1% increase in the TEI (3293 MJ/t clk) for the reference clinker-making plant.

Effect of [O_2] in Flue Gas. As noted previously solid AFs are unlikely to be fully combusted when the [O_2] in flue gas is only 1%, so the TEF model also assesses the increase in TEI under conditions where the flue gas [O_2] is greater than 1%. The energy required to maintain the same process temperature as the NG-based reference plant increases non-linearly with the [O_2] in the flue gas as illustrated in Fig. 6. To incorporate this non-linear trend with [O_2], the non-linear curve fit with a lower MAE than the linear curve fit was selected in **Eq. (2).** Increasing [O_2], from 1% to 2% in flue gas, increases the TEI by about 174 MJ/t clk (5.3% of the TEI of the reference clinker-making plant) while an increase from 2% to 3% in flue gas increases by about 258 MJ/t clk (7.8% of the TEI of the reference clinker-making plant).

Application of the Regression Equation. Given the potential increase in thermal energy intensity (TEI), if AFs needed to burn at higher [O_2] in flue gas, there could be several challenges in the clinker-making plant. For example, higher combustion air demand (Table 4, **R16**) in the pre-calciner compared to the reference case could affect the solid retention time. To address this technical challenge, the cement plant operator would have to find different measures such as an increase in turbulence inside the pre-calciner [46] or feeding air at multiple stages [47]. As the pre-calciner unit of the clinker-making plant studied here is new and tall enough to burn AFs completely (personal communication with the cement plant operator), this study has excluded the impact of change in airflow on the solid retention time.

However, changes in the TEI due to AF co-firing could increase the production cost. The regression equation presented here could easily predict the changes for a different type of AFs and various [O_2] in the flue gas, thereby facilitating the cement plant operator in decision-making.

For example, the use of AFs with the moisture content of 20% could increase the TEI by 62 MJ/t clk of which 31 MJ/t clk (50% GJ basis in pre-calciner) would have to be supplied from AFs. This means if wood dust with 20% moisture content is used, there will be a 3% increase in the amount (tonne/t clk) of wood dust supply (Table 3, **R4 and R8**) relative to the dry wood dust supply. Similarly, increasing [O_2] in flue gas from 1% to 3% increases the TEI by 432 MJ/t clinker of which 216 MJ/t clinker is from AFs. This means that the wood dust supply would be increased by 22% (Table 3, **R4 and R8**). Therefore, the regression equation could help the cement plant operator to design the AF conveying system and drying system that take into consideration the range of moisture, and to estimate the incremental clinker production cost.

In addition to this, the cement plant operator may also need to trade-off the energy required for grinding AFs and the excess air necessary to ensure complete combustion of larger particles of AFs. For instance, the specific grinding electricity, though it also depends on many other parameters such as type of grinder and type of AFs, increases from 58 to 672 kWh/tonne of dry wood when the particle size reduces from 1000 to 100 μm [48]. Therefore, having the developed regression equation would also help the cement plant operator to identify a cheaper option between the grinding energy and thermal energy cost, without running the complex thermal energy flow model.

4. Conclusions

The thermal energy flow (TEF) model developed here, for a cement plant with a 4-stage cyclone preheater, a vertical cylindrical pre-calciner and a rotary kiln, presents how the properties of alternative fuels (AFs) and oxygen concentration in flue gas affect the TEI, AD and CO_2 emissions when AFs with higher carbon intensities are introduced to replace 50% of pre-calciner GJ demand in a natural gas-fired cement plant. While the TEF model can assess the changes in energy and air flows for all kind of solid fuels co-firing with NG in the pre-calciner, it is difficult, time-consuming, and costly to run the TEF model for any new AF. Therefore, a regression equation was also devised to determine the TEI of the cement plant.

This study concludes that:

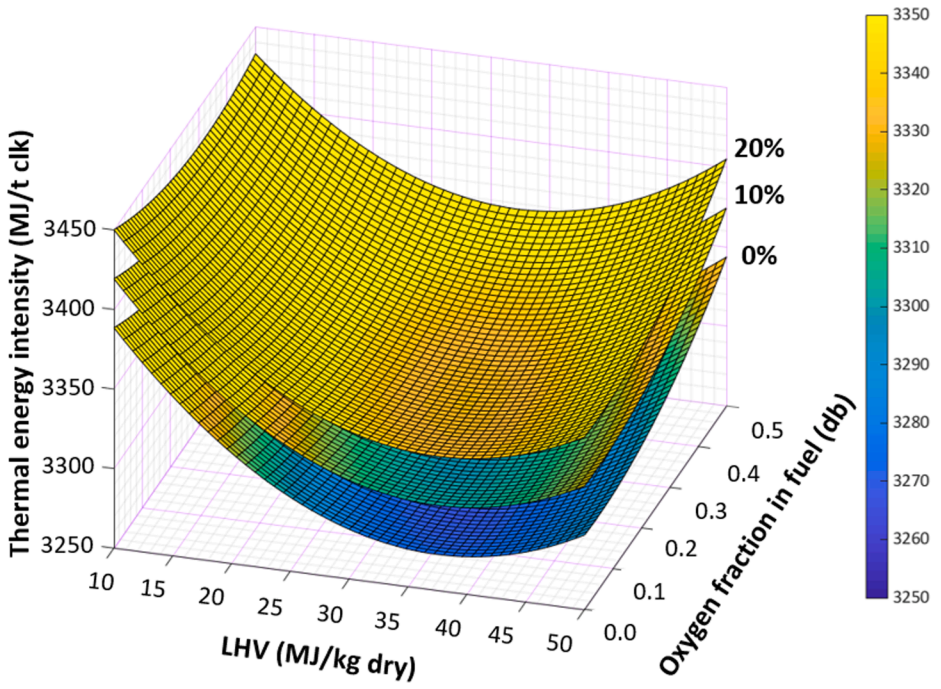

Fig. 5. The calculated effect of moisture content (0%, 10%, 20%) on thermal energy intensity for a range of values for alternative fuel's LHV and embedded elemental oxygen fraction in dry basis (db) ([O_2] at the exit of pre-calciner = 1%).

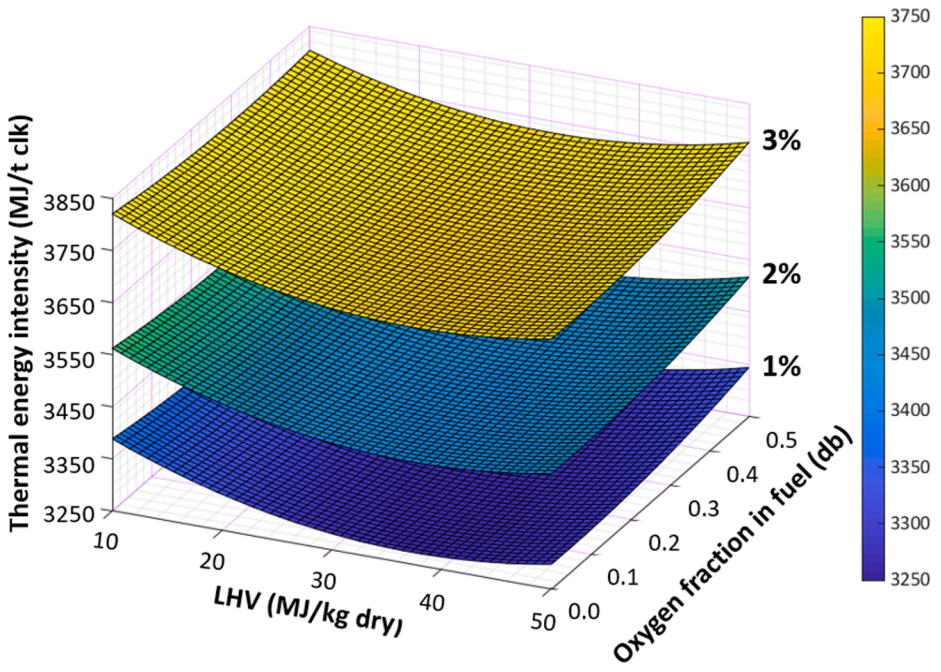

Fig. 6. The calculated effect of [O_2] in flue gas at the exit of pre-calciner (1%, 2%, 3%) on thermal energy intensity for a range of values for alternative fuel's LHV and embedded elemental oxygen fraction in dry basis (db) MC in AF = 0%).

- Replacing natural gas by AFs without increasing the [O_2] in the flue gas has little impact on thermal energy intensity (TEI) and total air demand (AD). However, to ensure complete combustion of solid fuels this option may not be available to the plant operator.
- Replacing natural gas by AFs and raising the [O_2] in flue gas from 1% to 3% increases the average AD by 334 Nm^3/t clk and TEI by 443 MJ/t clk, which are increases of 21% and 13%, respectively relative to the NG-based reference plant with 1% [O_2] in the flue gas.
- While moisture content of AFs is linearly coupled to increases in TEI (3.1 MJ/t clk for every 1% rise in AF moisture content), the increase in the flue gas [O_2] required to achieve complete combustion has a proportionately greater impact on TEI at higher flue gas [O_2] concentrations.
- Due to higher carbon intensity ($kgCO_2$/GJ) of AFs compared to the reference case fuel, the total CO_2 emissions intensity increases in the range of 1–8% and 4–14% when AFs are co-fired at 1% and 3% [O_2] in the flue gas, respectively.
- The use of carbon–neutral AFs such as wood dust at 3% [O_2] in the flue gas could avoid GHG emissions by up to 43 $kgCO_2$/t clk, equivalent to an emission reduction of 65,919 tCO_2 per year.
- The TEI regression equation validated using local AFs could quickly assess the performance of AF co-firing and then facilitate the cement plant operators to estimate the incremental cost of the clinker production.

This study shows that in a natural gas-fired cement plant, the use of AFs is likely to increase thermal energy intensity, air demand, electricity requirement and total CO_2 emissions. Only if the AFs are biogenic, would GHG emissions be reduced. The lower (or even negative) cost for AFs relative to natural gas may provide a justification for their use depending on the carbon price, the biogenic carbon content in AFs, fuel costs, electricity cost, and the emission benchmark for the cement plant.

CRediT authorship contribution statement

Daya R. Nhuchhen: Conceptualization, Modeling, Software. **Song P. Sit:** Validation. **David B. Layzell:** Conceptualization.

Declaration of Competing Interest

The authors declare that they have no known competing financial interests or personal relationships that could have appeared to influence the work reported in this paper.

Acknowledgements

The authors thank the LafargeHolcim Team at the Exshaw Cement Plant for their support in providing technical information and Mr. Rustam Punja from Geocycle Canada Inc. for data on the elemental composition of local waste materials in Alberta, Canada. We appreciate the valuable insights and advice provided by Mr. Sam Fujimoto (Process Environmental Consultant), and Dr. Darko Matovic (Professor, Queen University, Kingston). The funding for this work was provided to DBL from Alberta Innovates, Emissions Reduction Alberta, Natural Science and Engineering Research Council of Canada and LafargeHolcim Inc.

Appendix A:. Major reactions in clinker-making process

This section provides the major decomposition and mineral formation reactions in the pre-calciner and rotary kiln of the cement plant and a summary of the standard enthalpy of respective reactions.

Table A1
Major decomposition and mineral formation reactions and standard enthalpy of reaction 25 °C and atmospheric pressure.

SN	Reactions	Location	Standard enthalpy of reaction (Δh), kJ/mole
R1	$CaCO_3 \rightarrow CaO + CO_2$	Pre-calciner + Kiln	179.17
R2	$MgCO_3 \rightarrow MgO + CO_2$	Pre-calciner + Kiln	100.69
R3	$2CaO + SiO_2 \rightarrow 2(CaO).SiO_2 or C_2S$	Pre-calciner + Kiln	−127.46
R4	$4CaO + Al_2O_3 + Fe_2O_3 \rightarrow 4(CaO).Al_2O_3.Fe_2O_3 or C_4AF$	Kiln	−40.42
R5	$3CaO + Al_2O_3 \rightarrow 3(CaO).Al_2O_3 or C_3A$	Kiln	19.46
R6	$CaO + 2(CaO).SiO_2 \rightarrow 3(CaO).SiO_2 or C_3S$	Kiln	11.92

Appendix B:. Combustion analysis

B.1 Stoichiometric fuel combustion

Generic stoichiometric combustion equation for NG/AF co-firing can be expressed as:

$$X_{NG}\left\{n_1CH_4 + n_2C_2H_6 + n_3C_3H_8 + n_4(C_4H_{10})_{iso} + n_5(C_4H_{10})_n + n_6C_6H_{12} + n_7N_2 + n_8CO_2 + n_9H_2S\right\} + W_{AF}(w_1C + w_2H_2 + w_3O_2 + w_4N_2 + w_5Ar + w_6S + w_7Cl_2 + w_8H_2O) + \lambda_{s-NG/AF}\left(O_2 + \frac{a_{N_2}}{a_{O_2}}N_2 + \frac{a_{Ar}}{a_{O_2}}Ar + \frac{a_{H_2O}}{a_{O_2}}H_2O\right) = m_1CO_2 + m_2H_2O + m_3N_2 + m_4Ar + m_5SO_2 + m_6Cl_2 \quad (B.1)$$

where, n_i is the molar fraction of the various molecules in NG (kmole per kmole of NG), w_i is the molar fraction of the elemental and moisture compositions in AF (kmole per kg of AF), m_i is the molar flow rate of combustion products (kmole per unit time), X_{NG} is the molar flow rate of NG (kmole per unit time), W_{AF} is the mass flow rate of AF (kg per unit time), and $\lambda_{s-NG/AF}$ is the amount of oxygen required for the stoichiometric combustion, which is supplied through the air with compositions:

$$1kmole air = a_{N_2}N_2 + a_{O_2}O_2 + a_{Ar}Ar + a_{H_2O}(H_2O) \quad (B.1a)$$

where, a_i is the molar compositions of air (kmole per kmole of air). While the oxygen demand could be estimated by balancing oxygen atoms, the molar flow rate of flue gas at stoichiometric combustion condition was determined by adding combustion products of each fuel and other gases entered in the system via air. The mathematical analysis is presented in the supplementary **Section 4.1**. The simplified stoichiometric molar oxygen demand and flue gas flow rate can be expressed as:

$$\lambda_{s-NG/AF} = X_{NG}O_{2O_2/NG} + W_{AF}O_{2O_2/AF} \quad (B.1b)$$

where, $O_{2O_2/NG}$ and $O_{2O_2/AF}$ are the stoichiometric oxygen demand for NG and AF, respectively and can be estimated as:

$$O_{2O_2/NG} = (2n_1 + 3.5n_2 + 5n_3 + 6.5n_4 + 6.5n_5 + 9n_6 + 1.5n_9) \quad (B.1c)$$

$$O_{2O_2/AF} = (w_1 + 0.5w_2 - w_3 + w_6) \quad (B.1d)$$

The molar flow rate of flue gas from the stoichiometric combustion of natural gas and alternative fuel ($m_{t-s-NG/AF}$) can be estimated as:

$$m_{t-s-NG/AF} = X_{NG}C_{NG} + W_{AF}C_{AF} + \lambda_{s-NG/AF}C_{air} \quad (B.1e)$$

where, C_{NG}, C_{AF} and C_{air} are the constants associated with the properties of NG, AF and air, respectively and can be estimated as:

$$C_{NG} = (3n_1 + 5n_2 + 7n_3 + 9n_4 + 9n_5 + 12n_6 + n_7 + n_8 + 2n_9) \quad (B.1f)$$

$$C_{AF} = (w_1 + w_2 + w_4 + w_5 + w_6 + w_7 + w_8) \quad (B.1g)$$

$$C_{air} = \left(\frac{a_{H_2O}}{a_{O_2}} + \frac{a_{N_2}}{a_{O_2}} + \frac{a_{Ar}}{a_{O_2}}\right) \quad (B.1h)$$

B.2 Combustion in Kiln

Combustion of a fuel occurs at higher air supply than the stoichiometric air demand since the kiln passes the flue gas with 6.5% [O_2] onto the pre-calciner (Fig. 1). Therefore, the combustion equation in the rotary kiln, which could burn NG or AF along with the supplied air, can be expressed as:

$$X_{NG-K}\left\{n_1CH_4 + n_2C_2H_6 + n_3C_3H_8 + n_4(C_4H_{10})_{iso} + n_5(C_4H_{10})_n + n_6C_6H_{12} + n_7N_2 + n_8CO_2 + n_9H_2S\right\} + W_{AF-K}(w_1C + w_2H_2 + w_3O_2 + w_4N_2 + w_5Ar + w_6S + w_7Cl_2 + w_8H_2O) + C_{UB-C-K-i} + \lambda_{a-NG/AF-K}(1 + L_{lk-K})\left(O_2 + \frac{a_{N_2}}{a_{O_2}}N_2 + \frac{a_{Ar}}{a_{O_2}}Ar + \frac{a_{H_2O}}{a_{O_2}}H_2O\right) + n_{cal-K}CO_2 + \lambda_{s-NG/AF}O_{enrich-K}O_2 = m_1CO_2 + m_2H_2O + m_3N_2 + m_4Ar + m_5SO_2 + m_6Cl_2 + m_7CO + m_8O_2 \quad (B.2)$$

$C_{UB-C-K-i}$ is the amount of unburned solid carbon (kmole per unit time) entering in the kiln along with the calcined raw meal collected by the the bottom cyclone separator (Cy: V, see **Figure S1**). L_{lk-K} is the fraction of oxygen entering into the kiln in the form of a leakage air and is assumed to be proportional to the actual oxygen demand. n_{cal-K} is the amount of CO_2 (kmole per unit time) released from the calcination reaction in the kiln. $O_{enrich-K}$ is the term introduced in the model to examine oxygen-enriched combustion in the kiln, which is expressed as a fraction of stoichiometric oxygen requirement for fuel combustion. However, this study excludes cases of unburned solid carbon and oxygen enrichment. The mathematical analysis is presented in the supplementary **Section 4.2**. The simplified expression for the actual oxygen demand in the rotary kiln ($\lambda_{a-NG/AF-K}$) can be expressed as:

$$\lambda_{a-NG/AF-K}=\frac{1}{1+L_{lk-K}}\left\{\left(X_{NG-K}O_{2O_2/NG}+W_{AF-K}O_{2O_2/AF}\right)(1-O_{enrich-K})+C_{UB-C-K-i}-0.5\overline{CO}_K m_{t-a-NG/AF-K}+\overline{O_2}_K m_{t-a-NG/AF-K}\right\} \tag{B.2a}$$

where, $\overline{CO}_K$ and $\overline{O_2}_K$ are concentrations of CO and O_2 in the flue gas leaving rotary kiln, respectively and are considered as input model parameters. The actual molar flow rate of the total flue gas ($m_{t-a-NG/AF-K}$) from the rotary kiln can be evaluated as:

$$m_{t-a-NG/AF-K}=\frac{1}{(1-\overline{O_2}_K)}\left\{X_{NG-K}C_{NG}+W_{AF-K}C_{AF}+C_{UB-C-K-i}+\lambda_{a-NG/AF-K}(1+L_{lk-K})C_{air}+n_{cal-K}\right\} \tag{B.2b}$$

B.3 Combustion in pre-calciner

The actual combustion equation in pre-calciner, which could burn NG or AF along with air supplied and the kiln flue gas, can be expressed as:

$$\begin{aligned}&X_{NG-PC}\left\{n_1CH_4+n_2C_2H_6+n_3C_3H_8+n_4(C_4H_{10})_{iso}+n_5(C_4H_{10})_n+n_6C_6H_{12}+n_7N_2+n_8CO_2+n_9H_2S\right\}+W_{AF-PC}(w_1C+w_2H_2+w_3O_2+w_4N_2+w_5Ar+w_6S\\&+w_7Cl_2+w_8H_2O)+\lambda_{a-NG/AF-PC}(1+L_{lk-PC})\left(O_2+\frac{a_{N_2}}{a_{O_2}}N_2+\frac{a_{Ar}}{a_{O_2}}Ar+\frac{a_{H_2O}}{a_{O_2}}H_2O\right)+n_{fgk-CO_2}CO_2+n_{fgk-H_2O}H_2O+n_{fgk-CO}CO+n_{fgk-O_2}O_2+n_{fgk-N_2}N_2\\&+n_{fgk-Ar}Ar+n_{fgk-SO_2}SO_2+n_{fgk-Cl_2}Cl_2+n_{cal-PC}CO_2+\lambda_{s-NG/AF}O_{enrich-PC}O_2=m_1CO_2+m_2H_2O+m_3N_2+m_4Ar+m_5SO_2+m_6Cl_2+m_7CO+m_8O_2\\&+m_9C\end{aligned} \tag{B.3}$$

where, n_{fgk-i} is the molar flow rate of gases species in flue gas from the kiln. L_{lk-PC} is the fraction of oxygen entering into the pre-calciner in the form of a leakage air. n_{cal-PC} is the amount of CO_2 (kmole per unit time) released from the calcination reaction in the pre-calciner. $O_{enrich-PC}$ is the term introduced in the model to examine oxygen-enriched combustion in the pre-calciner. The mathematical analysis is presented in the supplementary **Section 4.3**. The simplified expression for the actual oxygen demand in the pre-calciner ($\lambda_{a-NG/AF-PC}$) can be expressed as:

$$\lambda_{a-NG/AF-PC}=\frac{1}{1+L_{lk-PC}}\left\{\left(X_{NG-PC}O_{2O_2/NG}+W_{AF-PC}O_{2O_2/AF}\right)(1-O_{enrich-PC})+0.5n_{fgk-CO}-0.5\overline{CO}_{PC}m_{t-a-NG/AF-PC}-m_9+\overline{O_2}_{PC}m_{t-a-NG/AF-PC}-n_{fgk-O_2}\right\} \tag{B.3a}$$

where, $\overline{CO}_{PC}$ and $\overline{O_2}_{PC}$ are concentrations of CO and O_2 in the flue gas leaving the pre-calciner, respectively and are considered as the model input parameters. The actual molar flow rate of the total flue gas leaving the pre-calciner ($m_{t-a-NG/AF-PC}$) can be estimated as:

$$m_{t-a-NG/AF-PC}=\frac{1}{1-\overline{O_2}_{PC}}\left\{X_{NG-PC}C_{NG}+W_{AF-PC}C_{AF}+\lambda_{a-NG/AF-PC}(1+L_{lk-PC})C_{air}+n_{fgk-CO_2}+n_{fgk-CO}+n_{fgk-H_2O}+n_{fgk-N_2}+n_{fgk-Ar}+n_{fgk-SO_2}+n_{fgk-Cl_2}+n_{cal-PC}-m_9\right\} \tag{B.3b}$$

Appendix C:. Expressions for fuel flow rate in the kiln and pre-calciner

C.1 Rotary Kiln

The energy balance in the rotary kiln would help to determine the thermal energy intensity (Q_{F-K}) and corresponding fuel (F) demands (m_{NG-K} *or* W_{AF-K}). Assuming there is no alternative fuel combustion, the total mass flow rate of NG in the rotary kiln (m_{NG-K}) can be determined as:

$$m_{NG-K}=\frac{Q_{F-K}}{C_{p-NG-K}\left(T_{NG-K-i}-T_{ref}\right)+LHV_{NG}\beta_{NG-K}} \tag{C.1}$$

where, LHV_{NG} is the lower heating value of NG, β_{NG-K} is the carbon conversion factor of NG in the kiln, C_{p-NG-K} is the specific heat capacity of NG at kiln's operating condition, T_{NG-K-i} is the temperature of NG at the inlet the kiln (assumed 25 °C in this study), and T_{ref} is the reference temperature condition.

C.2 Pre-calciner

In the pre-calciner, the thermal energy demand (Q_{F-PC}) is supported by combustion of AF and NG, so we can determine the mass flow rate of AF (W_{AF-PC}) and NG (m_{NG-PC}) as:

$$W_{AF-PC} = \frac{\theta_{AF-PC} Q_{F-PC}}{(1 - M_{w-AF}) C_{p-AF-PC} \left(T_{AF-PC-i} - T_{ref}\right) + M_{w-AF} \left(h_{AF-PC-i} - h_{ref}\right) + LHV_{AF} \beta_{AF-PC}} \quad \text{(C.2a)}$$

$$m_{NG-PC} = \frac{(1 - \theta_{AF-PC}) Q_{F-PC}}{C_{p-NG-PC} \left(T_{NG-PC-i} - T_{ref}\right) + LHV_{NG} \beta_{NG-PC}} \quad \text{(C.2b)}$$

where, θ_{AF-PC} is the fraction of thermal energy demand in the pre-calciner supported by the combustion of alternative fuels. β_{NG-PC} and β_{AF-PC} are the carbon conversion factor of NG and AF in the pre-calciner, respectively. $T_{NG-PC-i}$ and $T_{AF-PC-i}$ are the temperature of NG and AF, respectively at the inlet of the pre-calciner (assumed 25 °C in this study). M_{w-AF} is the amount of moisture in AF, $h_{AF-PC-i}$ is the mass enthalpy of moisture at the inlet temperature and pressure conditions and h_{ref} is the enthalpy of moisture at the reference conditions.

Appendix D:. Shomate equation

The temperature-dependent Shomate equation [28] can be expressed as:

$$C_p = A + Bt + Ct^2 + Dt^3 + E/t^2 \quad \text{(D.1)}$$

where, C_p is the specific heat capacity (J/mol K), t is the temperature (K)/1000, and A *to* E are the constants [29] specific to each gas molecules and are presented in **Table S3** in the supplementary file.

Appendix E. Supplementary data

Supplementary data to this article can be found online at https://doi.org/10.1016/j.fuel.2021.120544.

References

[1] Andrew RM. Global CO_2 emissions from cement production. Earth Syst Sci Data 2018;10(1):195–217. https://doi.org/10.5194/essd-10-195-2018.

[2] IEA. Technology Roadmap - Low-Carbon Transition in the Cement Industry. International Energy Agency, 2018. Retrieved online at https://www.iea.org/publications/freepublications/publication/TechnologyRoadmapLowCarbonTransitionintheCementIndustry.pdf.

[3] de Pee A, Pinner D, Reolofsen O, Somers K, Eveline S, Witteveen, M. Decarbonization of Industrial Sectors: The Next Frontier. McKinsey & Company, 2018. Retrieved online at https://www.mckinsey.com/industries/oil-and-gas/our-insights/decarbonization-of-industrial-sectors-the-next-frontier.

[4] Pardo N, Moya JA, Mercier A. Prospective on the energy efficiency and CO2 emissions in the EU cement industry. Energy 2011;36(5):3244–54. https://doi.org/10.1016/j.energy.2011.03.016.

[5] Naqi A, Jang J. Recent progress in green cement technology utilizing low-carbon emission fuels and raw materials: A review. Sustainability 2019;11:537–55. https://doi.org/10.3390/su11020537.

[6] Ariyaratne WKH, Melaaen MC, Tokheim LA. The effect of alternative fuel combustion in the cement kiln main burner on production capacity and improvement with oxygen enrichment. Int J Mater Metall Eng, 2013;7(4):185–91. Retrieved online at https://publications.waset.org/13206/the-effect-of-alternative-fuel-combustion-in-the-cement-kiln-main-burner-on-production-capacity-and-improvement-with-oxygen-enrichment.

[7] Bourtsalas AC, Zhang J, Castaldi MJ, Themelis NJ. Use of non-recycled plastics and paper as alternative fuel in cement production. J Cleaner Prod 2018;181:8–16. https://doi.org/10.1016/j.jclepro.2018.01.214.

[8] Ngadi Z, Lahlaouti ML. Impact of using alternative fuels on cement rotary kilns: Experimental study and modeling. Procedia Eng 2017;181:777–84. https://doi.org/10.1016/j.proeng.2017.02.465.

[9] Brunner PH, Rechberger H. Waste to energy – key element for sustainable waste management. Waste Manage 2015;37:3–12. https://doi.org/10.1016/j.wasman.2014.02.003.

[10] Cherubini F, Bargigli S, Ulgiati S. Life cycle assessment (LCA) of waste management strategies: Landfilling, sorting plant and incineration. Energy 2009;34(12):2116–23. https://doi.org/10.1016/j.energy.2008.08.023.

[11] Tsiliyannis CA. Alternative fuels in cement manufacturing: Modeling for process optimization under direct and compound operation. Fuel 2012;99:20–39. https://doi.org/10.1016/j.fuel.2012.03.036.

[12] Rahman A, Rasul M, Khan MMK, Sharma S. Assessment of energy performance and emission control using alternative fuels in cement industry through a process model. Energies 2017; 10: 1996-1-1996-17. 10.3390/en10121996.

[13] Tsiliyannis CA. Cement manufacturing using alternative fuels: Enhanced productivity and environmental compliance via oxygen enrichment. Energy 2016;113:1202–18. https://doi.org/10.1016/j.energy.2016.07.082.

[14] Akhtar S, Ervin E, Raza S, Abbas T. From coal to natural gas: Its impact on kiln production, clinker quality and emissions. IEEE Trans Industry Appl 2016;52(2):1913–24. https://doi.org/10.1109/TIA.2015.2504554.

[15] Price L, Sinton J, Worrell E, Phylipsen D, Xiulian H, Ji L. Energy use and carbon dioxide emissions from steel production in China. Energy 2002;27(5):429–46. https://doi.org/10.1016/S0360-5442(01)00095-0.

[16] Atsonios K, Grammelis P, Antiohos SK, Nikolopoulos N, Kakaras E. Integration of calcium looping technology in existing cement plant for CO2 capture: Process modeling and technical considerations. Fuel 2015;153:210–23. https://doi.org/10.1016/j.fuel.2015.02.084.

[17] Government of Alberta. Technology Innovation and Emissions Reduction Regulation. Alberta Queen's Printer, 2019. Retrieved online at http://www.qp.alberta.ca/1266.cfm?page=2019_133.cfm&leg_type=Regs&isbncln.

[18] Government of Canada. A Healthy Environment and A Healthy Economy: Canada's Strengthened Climate Plan to Create Jobs and Support People, Communities and the Planet. Environment and Climate Change Canada, 2020. Retrieved online at https://www.canada.ca/content/dam/eccc/documents/pdf/climate-change/climate-plan/healthy_environment_healthy_economy_plan.pdf.

[19] LafargeHolcim. The 2030 Plan - Building for Tomorrow. LafargeHolcim, 2016. Retrieved online at https://www.lafargeholcim.com/2030-plan.

[20] ECN. Phyllis2 - Database for the physico-chemical composition of (treated) lignocellulosic biomass, micro- and macroalgae, various feedstocks for biogas production and biochar. Energy Research Center of the Netherlands, 2019. Retrieved online at https://phyllis.nl/.

[21] Bergman R, Puettmann M, Taylor A, Skog KE. The carbon impacts of wood products. Forest Product Journals 2014; 64: 220–231. 10.13073/FPJ-D-14-00047.

[22] Gorski J, Israel B. Life Cycle Assessment of Low-Carbon Fuels: Lafarge Exshaw Cement Plant Kiln 6-Greenhouse Gas Emissions Life Cycle Assessment (version A). The Pembina Institute, 2018. Retrieved online at https://lafargeexshaw.ca/wp-content/uploads/2019/01/2018-Lafarge-LCA-Final-Report-GHGs-rA.pdf.

[23] Larsen AW, Fuglsang K, Pedersen NH, Fellner J, Rechberger H, Astrup T. Biogenic carbon in combustible waste: Waste composition, variability and measurement uncertainty. Waste Management & Research: The Journal for Sustainable Circular Economy 2013;31(10):56–66. https://doi.org/10.1177/0734242X13502387.

[24] Benhelal E, Rafiei A. Overview of process modeling software: Utilizing alternative fuels in cement plant for air pollution reduction. Energy Science and Technology 2012; 4(1): 10-18. Retrieved online at http://citeseerx.ist.psu.edu/viewdoc/download?doi=10.1.1.826.4946&rep=rep1&type=pdf.

[25] Gao T, Shen L, Shen M, Liu L, Chen F. Analysis of material flow and consumption in cement production process. J Cleaner Prod 2016;112(1):553–65. https://doi.org/10.1016/j.jclepro.2015.08.054.

[26] Kabir G, Abubakar AI, El-Nafaty UA. Energy audit and conservation opportunities for pyroprocessing unit of a typical dry process cement plant. Energy 2010;35(3):1237–43. https://doi.org/10.1016/j.energy.2009.11.003.

[27] Politecnico di Milano. Design and Performance of CEMCAO Cement Plant Without CO2 Capture. CEMCAP, 2016. Retrieved online at https://zenodo.org/record/1001664#.XFTPj1xKiUk.

[28] Linstrom PJ. A Guide to the NIST Chemistry WebBook. National Institute of Standards and Technology, 2016. https://webbook.nist.gov/chemistry/guide/.

[29] Chase MW. NIST-JANAF Thermochemical Tables, Fourth Edition. Journal of Physical and Chemical Reference Data, Monograph 1998; 9: 1–1951.

[30] Matschei T, Lothenbach B, Glasser FP. Thermodynamic properties of Portland cement hydrates in the system CaO–Al2O3–SiO2–CaSO4–CaCO3–H2O. Cem Concr Res 2007;37(10):1379–410. https://doi.org/10.1016/j.cemconres.2007.06.002.

[31] Green RH, Perry DW. Perry's Chemical Engineers' Handbook. eighth ed. USA: McGraw-Hill Companies Inc.; 2008.

[32] Lafarge Exshaw. Reports | Lafarge Exshaw: Lafarge Low Carbon Fuel Projects. LafargeHolcim Inc, 2019. Retrieved online at https://lafargeexshaw.ca/reports/.

[33] CCME. National Emission Guidelines for Cement Kilns. Canadian Council of Ministers of the Environment, Winnipeg, Canada, 1998. Retrieved online at https://www.ccme.ca/files/Resources/air/emissions/pn_1284_e.pdf.
[34] KHD. Burning Technology: PYROCLON Calciner. KHD, 2012. Retrieved online at https://www.khd.com/tl_files/downloads/products/burning-technology/kiln-system/calcinersystems/khd_burningtechnology_pyroclon.pdf.
[35] De Lena E, Spinelli M, Gatti M, Scaccabarozzi R, Campanari S, Consonni S, et al. Techno-economic analysis of calcium looping processes for low CO2 emission cement plants. Int J Greenhouse Gas Control 2019;82:244–60. https://doi.org/10.1016/j.ijggc.2019.01.005.
[36] Gibbs MJ, Soyka P, Conneely D. Good Practice Guidance and Uncertainty Managment in National Greenhouse Gas Inventories: CO2 Emissions from Cement Production. Intergovernmental Panel on Climate Change 2001. Retrieved online at https://www.ipcc-nggip.iges.or.jp/public/gp/bgp/3_1_Cement_Production.pdf.
[37] Worrell E, Price L, Martin N, Hendriks C, Meida LO. Carbon dioxide emissions from the global cement industry. Annu Rev Energy Env 2001;26(1):303–29. https://doi.org/10.1146/annurev.energy.26.1.303.
[38] NRC. Canadian Cement Industry Energy Benchmarking: Summary Report. Natural Resources Canada, Canadian Industry Program for Energy Conservation (CIPEC), 2009. Retrieved online at https://www.nrcan.gc.ca/sites/www.nrcan.gc.ca/files/oee/pdf/Publications/industrial/cement-eng.pdf.
[39] Farag LM. Energy and exergy analysis of Egyptian cement kiln plant with complete kiln gas diversion through bypass. Int J Adv Appl Sci 2012;1(2):35–44. Retrieved online at https://www.semanticscholar.org/paper/Energy-and-Exergy-Analyses-of-Egyptian-Cement-Kiln-Farag/ac02be9b37f84cc7229f48270fe99b19396cf546.
[40] Khurana S, Banerjee R, Gaitonde U. Energy balance and cogeneration for a cement plant. Appl Therm Eng 2002;22(5):485–94. https://doi.org/10.1016/S1359-4311(01)00128-4.
[41] Kolip A, Savas AF. Energy and exergy analyses of a parallel flow, four-stage cyclone precalciner type cement plant. Int J Phys Sci 2010;5(7):1147–63. Retrieved online at https://academicjournals.org/journal/IJPS/article-full-text-pdf/FB76B7828727.
[42] Summerbell DL, Barlow CY, Cullen JM. Potential reduction of carbon emissions by performance improvement: A cement industry case study. J Cleaner Prod 2016;135:1327–39. https://doi.org/10.1016/j.jclepro.2016.06.155.
[43] Nie Y, Zhang S, Liu RE, Roda-Stuart DJ, Ravikumar AP, Bradley A, et al. Greenhouse-gas emissions of Canadian liquefied natural gas for use in China: Comparison and synthesis of three independent life cycle assessments. J Cleaner Prod 2020;258:120701–12. https://doi.org/10.1016/j.jclepro.2020.120701.
[44] ECCC. National Inventory Report 1990 –2018: Greenhouse Gas Sources and Sinks in Canada. Environment and Climate Change Canada, Canada, 2020. Retrieved online at http://www.publications.gc.ca/site/eng/9.506002/publication.html.
[45] Mokrzycki E, Uliasz- Bocheńczyk A. Alternative fuels for the cement industry. Appl Energy 2003;74:95–100. https://doi.org/10.1016/S0306-2619(02)00135-6.
[46] Fande MA, Joshi MPV, Gabhane MS, Sahu MMK. CFD investigation of combustion in 660MW tangential fired boiler. Int J Eng Res Tech 2014;3(1):892-908. Retrieved online at https://www.ijert.org/research/cfd-investigation-of-combustion-in-660mw-tangential-fired-boiler-IJERTV3IS10356.pdf.
[47] Nosek R, Holubčík M, Papučík S. Emission controls using different temperatures of combustion air. The Scientific World Journal 2014; 2014: Article ID 487549, 6 pages, 2014. https:/doi.org/10.1155/2014/487549.
[48] Wang J, Gao J, Brandt KL, Wolcott MP. Energy consumption of two-stage fine grinding of Douglas-fir wood. J Wood Sci 2018;64(4):338–46. https://doi.org/10.1007/s10086-018-1712-1.